JPET Fast Forward. Published on April 2, 2013 as DOI: 10.1124/jpet.113.203620

JPET #203620

TITLE PAGE

HCN1 channels as targets for anesthetic and non-anesthetic propofol analogs in the amelioration of mechanical and thermal hyperalgesia in a mouse model of neuropathic pain

Gareth R. Tibbs, Thomas J. Rowley, R. Lea Sanford, Karl F. Herold, Alex Proekt, Hugh C. Hemmings, Olaf S. Andersen, Peter A. Goldstein, Pamela D. Flood

Department of Anesthesiology, College of Physicians & Surgeons, Columbia University, New York, NY 10032 (GRT, TJR, PDF); Departments of Anesthesiology (KFH, AP, HCH, PAG), Pharmacology (HCH), and Physiology and Biophysics (RLS, OSA) Weill Cornell Medical College, New York, NY 10065

JPET Fast Forward. Published on April 2, 2013 as DOI: 10.1124/jpet.113.203620
This article has not been copyedited and formatted. The final version may differ from this version.

JPET #203620

RUNNING TITLE PAGE

Running Title	Propofol analogs and neuropathic pain

Corresponding Author

Peter A. Goldstein, MD
Department of Anesthesiology
Weill Cornell Medical College
1300 York Avenue, Room A-1050
New York, NY 10065

Phone (212) 746-5325
Fax (212) 746-4987
Email pag2014@med.cornell.edu

Text Pages (not including title page, abstract, references, legends or supplemental information)	:	24
Tables	:	1
Figures	:	6 + 5 Supplemental
References	:	59
Abstract	:	249
Introduction	:	597
Discussion	:	1,462

Abbreviations: ANTS: 8-aminonaphthalene-1,3,6-trisulfonic acid; 2,4-DSBP: 2,4-di-*sec*-butylphenol; 2,6-DSBP: 2,6-di-*sec*-butylphenol; $GABA_A$-R: type A GABA receptor; 2,4-DTBP: 2,4-di-*tert*-butylphenol; 2,6-DTBP: 2,6-di-*tert*-butylphenol; DHßCD: dihydroxy-ß-cyclodextrin; HCN: hyperpolarization-activated, cyclic nucleotide-regulated channel; $HPWL_{IPSI}$ and $HPWL_{CONTRA}$: Hind paw withdrawal latency of the ipsilateral and contralateral paws, respectively; LUVs: Large unilamellar vesicles; PNL: Partial sciatic nerve ligation; $P_{W,IPSI}$ and $P_{W,CONTRA}$: Probability of withdrawal of the ipsilateral and contralateral paws, respectively; TEVC: Two microelectrode voltage clamp.

Recommended Section Assignment: Behavioral Pharmacology

JPET Fast Forward. Published on April 2, 2013 as DOI: 10.1124/jpet.113.203620
This article has not been copyedited and formatted. The final version may differ from this version.

ABSTRACT

Chronic pain after peripheral nerve injury is associated with afferent hyper-excitability and upregulation of HCN-mediated (hyperpolarization-activated, cyclic nucleotide-regulated) I_H pacemaker currents in sensory neurons. HCN channels thus constitute an attractive target for treating chronic pain. HCN channels are ubiquitously expressed; analgesics targeting HCN1-rich cells in the PNS must spare the cardiac pacemaker current (carried mostly by HCN2 and 4) and the CNS (where all four isoforms are expressed). The alkylphenol general anesthetic propofol (2,6-di-iso-propylphenol) selectively inhibits HCN1 channels versus HCN2-4 and exhibits a modest pharmacokinetic preference for the periphery. Consequently, we hypothesized that propofol, and congeners, should be antihyperalgesic. Alkyl-substituted propofol analogs have different rank-order potencies with respect to HCN1 inhibition, $GABA_A$ receptor ($GABA_A$-R) potentiation and general anesthesia. Thus, 2,6- and 2,4-di-*tert*-butylphenol (2,6- and 2,4-DTBP) are more potent HCN1 antagonists than propofol while 2,6- and 2,4-di-*sec*-butylphenol (2,6- and 2,4-DSBP) are less potent. In contrast, DSBPs, but not DTBPs, enhance $GABA_A$-R function and are general anesthetics. 2,6-DTBP retained propofol's selectivity for HCN1 over HCN2-4. In a peripheral nerve ligation model of neuropathic pain, 2,6-DTBP and subhypnotic propofol are antihyperalgesic. The findings are consistent with these alkylphenols exerting analgesia *via* non-$GABA_A$-R targets and suggest that antagonism of central HCN1 channels may be of limited importance to general anesthesia. Alkylphenols are hydrophobic, and thus potential modifiers of lipid bilayers, but their effects on HCN channels are due to direct drug-channel interactions as they have little bilayer-modifying effect at therapeutic concentrations. The alkylphenol antihyperalgesic target may be HCN1 channels in the damaged PNS.

JPET Fast Forward. Published on April 2, 2013 as DOI: 10.1124/jpet.113.203620
This article has not been copyedited and formatted. The final version may differ from this version.

INTRODUCTION

Sensitization of the peripheral or central nervous system following injury can produce neuropathic pain, which manifests as allodynia, hyperalgesia, and/or spontaneous pain (Costigan et al., 2009). Neuropathic pain has an all-cause incidence rate of ~5% (Costigan et al., 2009) and is often refractory to treatment - or treatment has unacceptable side effects (Dray, 2008; Jensen et al., 2009). Neuropathic pain thus represents a significant public health issue, making it important to identify possible therapeutic targets and drugs that selectively act on those targets (Dray, 2008; Costigan et al., 2009).

In animal models of neuropathic pain, hyperexcitability and ectopic activity in primary afferents contribute to peripheral sensitization (Dray, 2008; Costigan et al., 2009; Dib-Hajj et al., 2009). These effects appear to be due, in part, to changes in HCN channel expression and function. First, *in situ* hybridization (Kouranova et al., 2008), immunohistochemical (Tu et al., 2004; Jiang et al., 2008; Kouranova et al., 2008), and electrophysiological (Mayer and Westbrook, 1983; Kouranova et al., 2008; Momin et al., 2008) data show that sensory neurons express HCN channels, and that injury causes altered HCN subunit trafficking (Chaplan et al., 2003; Jiang et al., 2008), and enhanced I_H current amplitudes (Chaplan et al., 2003; Yao et al., 2003). Second, sensory cell hyperexcitability is inhibited by superfusion with ZD7288 (Chaplan et al., 2003; Yao et al., 2003; Jiang et al., 2008), a selective pan-isoform inhibitor of HCN channels, and systemic, but not central, administration of ZD7288 alleviates mechanical allodynia (Chaplan et al., 2003; Lee et al., 2005). Third, HCN1 gene deletion partially blocks development of cold allodynia (Orio et al., 2009), and in a parallel fashion targeted deletion of HCN2 prevents the development of neuropathic pain in response to chronic nerve constriction

JPET Fast Forward. Published on April 2, 2013 as DOI: 10.1124/jpet.113.203620
This article has not been copyedited and formatted. The final version may differ from this version.

(Emery et al., 2011). These observations suggest that the HCN channels underlying I_H in peripheral neurons may represent a target for treatment of neuropathic pain (Emery et al., 2012).

Given the primacy of HCN2 and 4 in the cardiac current, analgesics that target I_H should preferentially inhibit channels comprised of, or containing, the HCN1 isoform and be restricted to the periphery (thereby sparing I_H in central neurons, including those that rely on the HCN1 isoform). The intravenous general anesthetic propofol (2,6-di-isopropylphenol) preferentially inhibits HCN1 with respect to HCN2, 3 and 4 (Cacheaux et al., 2005; Chen et al., 2005) and has a modest pharmacokinetic preference for the periphery (*i.e.*, plasma levels associated with anesthesia are higher than those in CSF: Table 1). However, its hypnotic properties and its potentiation of $GABA_A$-R activity (Franks, 2008) limit its routine use as an analgesic, even at low concentrations.

The 2,6- and 2,4- di-*sec*-butylphenol analogs of propofol (2,6-DSBP and 2,4-DSBP, respectively) potentiate $GABA_A$-Rs and act as general anesthetics, but the di-*tert* versions (2,6- and 2,4-DTBP) do neither (James and Glen, 1980; Krasowski et al., 2001). This steric specificity has been interpreted as, and is consistent with, the pharmacological and behavioral effects arising from an association of alkylphenols with a sterically-defined pocket on $GABA_A$-Rs (Krasowski et al., 2001).

We therefore examined the relative inhibitory potencies of the 2,6- and 2,4-dibutylphenols on HCN1. DSBPs were less potent than DTBP analogs, with 2,6-DTBP being the most potent inhibitor of HCN1 channels - with little effect on the other HCN isoforms. We also examined propofol (at subhypnotic doses) and 2,6,-DTBP in a mouse model of neuropathic pain; both are analgesic. Finally, we tested whether the hydrophobic alkylphenols alter lipid bilayer properties. The butylphenols modestly do this, but not at pharmacologically or

behaviorally relevant concentrations; propofol does not alter bilayer properties at the concentrations tested (up to 100 μM).

METHODS

Surgical procedures and drug administration With approval of the animal care committee at Columbia University, adult female C57 Black/6J mice (16 to 24 weeks old) were subject to partial sciatic nerve ligation (PNL (Seltzer et al., 1990)) according to institutional and Federal guidelines. In brief, following induction of isoflurane (2.5-3%) anesthesia, surgical incisions were made in the upper aspect of both the left and right hind limbs. In the left limb, approximately half of the nerve was ligated using an 8.0 braided silk suture (SofSilk, Coviden, Mansfield, MA). The nerve in the right limb was subject to similar mechanical manipulation but no suture was applied. Mice tended to exhibit protective behavior toward the ipsilateral paw, but their behavior was otherwise normal. Accordingly, and in keeping with the approved protocol, no therapeutic agents other than the indicated experimental test compounds were administered.

To examine 2,6-DTBP bioavailability, surgically-naïve mice received dihydroxy-ß-cyclodextrin (DHßCD) solubilized 2,6-DTBP (see Supplemental Methods for details), DHßCD alone or saline by intraperitoneal (*i.p.*) injection with a dosing schedule as per behavioral testing. 10-60 min after receipt of the appropriate final dose, mice were anesthetized with 2.5-3% isoflurane then exsanguinated by venous puncture. Blood concentration of 2,6-DTBP was determined by gas chromatography (GC see Supplemental Methods for details and Figures S1 and S2). To consider the toxicity of a high acute therapeutic dose of 2,6-DTBP, some animals received a single bolus of 80 mg/kg. The general condition of all of these animals was followed by qualitative observation of behavior (grooming and exploration) and survival. All animals were sacrificed within 7 days after receipt of a 2,6-DTBP/DHßCD injection.

For electrophysiology experiments, *Xenopus* oocytes were harvested from frogs anesthetized by immersion in ice-cold pH 7 buffered (sodium phosphate) 0.05% Tricane according institutional and Federal guidelines.

Behavioral testing To monitor the sensitivity of ipsilateral and contralateral hind paws to mechanical and thermal stimuli, mice were subjected to Von Frey fiber and thermal latency stimulus-response analysis using calibrated Von Frey fibers and a timed, tightly focused, variable intensity infrared heat source with an Hargreaves apparatus (IITC Life Science Inc., Woodland Hills, CA) as described previously (Udesky et al., 2005). Briefly, for each test, an animal was separately placed within a 132 cm^2 open-topped clear Plexiglas corral on the appropriate surface (a plastic-coated grid with a mesh size of 6 mm or a clear glass thermally regulated platform for the Von Frey and latency analyses, respectively) to which they had been previously acclimated and were allowed to settle for at least 10 min. Tests were performed on the plantar surface of both left and right hind paws. In the Von Frey analysis, the probability of paw withdrawal (P_W) was obtained by determining how many of 10 trials with a particular fiber resulted in the tested paw being withdrawn. Ipsilateral and contralateral paws were sequentially tested with a single fiber - with fiber strengths of 0.05, 0.4, 0.6, 1.1, 2.5, 3.3 and 4 g tested from weakest to strongest. In the thermal sensitivity analysis, the mean hind paw withdrawal latency (HPWL) was obtained by averaging the latency observed in five separate trials at a particular setting of the heat source. HPWL tests were done with alternating testing of the ipsilateral and contralateral paws. The response to heat source settings of 3 to 30% (in 3% increments, where 100% represents 150 Watts) was tested in a random order. If the paw was not withdrawn within 30 s the trial was terminated and a latency of 30 s noted.

Von Frey fibers exerting 2.5, 3.3 and 4 g yielded optimal discrimination of mechanical neuropathic hyperalgesia with respect to nociception (see Figure S3 in Supplemental Results). Thus, these fibers tended to produce withdrawal probabilities greater than 0 in the contralateral paw but less than 1 in the ipsilateral paw (Figures 1A, 4A, and S3) with the ratio of $P_{W,IPSI}$ / $P_{W,CONTRA}$ being similar at each stimulus intensity (2.9 ± 0.3, 2.9 ± 0.4 and 2.7 ± 0.2, respectively). Accordingly, we use the mean values of P_W ratios over these three stimuli to obtain a single, better defined, value of the ratio for each mouse at each time point and drug condition. To examine further the mechanical response we performed a Logit transformation (Ln [P_W/(1-P_W)]) of the withdrawal probability at each stimulus strength and then determined ES_{50}, the stimulus strength required for a Pw of 0.5 using Equation 1. Here, b_0 and b_1 are, respectively, the ordinate intercept and the slope of a regression through the Logit values plotted versus stimulus strength (*e.g.*, Figure 1C).

$$(1) \qquad ES_{50} = -b_{01}/b_1$$

To avoid skewing the data by omitting undefined values (Logit is not defined at a P_W of 0 or 1) we assigned such determinations values of 0.01 and 0.99 for the purpose of this transformation.

A heat lamp setting of 15% was optimal for examining thermal hyperalgesia rather than nociception (see Figure S4 in Supplemental Results). Thus, latencies in both ipsilateral and contralateral paws fell between our fastest and slowest detection thresholds (some 2-3 and 30 s, respectively) while the ratio $HPWL_{IPSI}$ / $HPWL_{CONTRA}$ was lowest at 15%. In contrast, 30% stimulation produced a largely, albeit not completely, nociceptive response in injured and uninjured paws, thereby providing data on anti-nociception.

JPET Fast Forward. Published on April 2, 2013 as DOI: 10.1124/jpet.113.203620
This article has not been copyedited and formatted. The final version may differ from this version.

Based on the above observations, we established an objective set of inclusion criteria to identify animals that developed mechanical and thermal neuropathic responses. For an animal to be included in the Von Frey mechanical analysis control values yielding $P_{W,IPSI} / P_{W,CONTRA} > 1$ and $P_{W,IPSI}$ at 4 g $\geq$ 0.3 were required; for inclusion in the HPWL thermal analysis the control $HPWL_{IPSI} / HPWL_{CONTRA}$ at 15% had to be $\leq$ 0.8; the majority of mice that recovered from PNL surgery developed robust and stable mechanical and thermal neuropathic responses.

To examine the influence of alkylphenols and/or vehicle on nocifensive behavior, we constructed cumulative dose response relationships wherein an aliquot of agent was administered each 60 min. Following each *i.p.* injection, animals were allowed to recover for 10 min then their behavior assayed during the subsequent 50 min. To maximize the sensitivity of our assay while minimizing the duration of the injection/monitoring cycles, and hence of drug clearance, we only examined lamp settings of 15 and 30% and fiber strengths of 0.6, 1.1, 2.5, 3.3 and 4 g during such drug trials. The reported dose of administered agents assumes no clearance of compound during the analysis. Drug trials were performed 7-17 days after PNL surgery (see Figures S3 and S4 in the Supplementary File).

Molecular Biology cDNA encoding murine HCN1, 2, and 4 and human HCN3 channels were subcloned into pGH19 (HCN1 and 4) or pGHE (HCN2 and HCN3) vectors and amplified in STBL2 cells (Invitrogen Corporation, Carlsbad, CA). cRNA was transcribed from NheI (HCN1, HCN3 and HCN4) or SphI (HCN2) linearized DNA using T7 RNA polymerase (Message Machine; Ambion, Houston, TX). 1-50 ng RNA was injected into each *Xenopus* oocyte.

JPET Fast Forward. Published on April 2, 2013 as DOI: 10.1124/jpet.113.203620
This article has not been copyedited and formatted. The final version may differ from this version.

Electrophysiology Recordings were made from *Xenopus* oocytes 2-5 days after cRNA injection. Cells were maintained in L-15 media without ficoll (Specialty Media, Phillipsburg, NJ) at 17 ^{o}C until use. Two microelectrode voltage clamp (TEVC) data, acquired using a Warner Instruments (Hamden, CT) OC-725C amplifier, were recorded with Pulse software (HEKA Elektronik, Lambrecht/Pfalz, Germany) following filtering at 2.5 kHz (Frequency Devices 902 8-pole Bessel filter) and digitization at 5 kHz using an ITC-18 interface (Instrutech Corporation, Port Washington, NY).

Microelectrodes were fabricated from 1B120-F4 borosilicate glass (World Precision Instruments, Sarasota, FL) with resistances of 0.1-0.5 MΩ (I passing) and 1-4 MΩ (V sensing) when filled with 3 M KCl. The Ag-AgCl ground wire(s) of the active virtual ground circuit were connected to the bath solution by 3M KCl-2% agar salt bridges placed downstream of, but close to, the oocyte. Recordings were obtained at room temperature (22-24 ^{o}C). In all cases the observed potential was within 1% of the reported command potential. For HCN1 and 2, oocytes were bathed in a recording solution of (in mM): 107 NaCl, 5 KCl, 2 MgCl2, 10 HEPES-free acid pH 7.4 (NaOH). For the poorly expressing HCN3 and 4 channels, the KCl concentration was raised to 25 mM by isoosmolar substitution of NaCl. In all recordings, the holding potential was -30 mV and the tail potential 0 mV.

To analyze the effects of alkylphenols on HCN channel gating, we constructed isochronal activation curves. In brief, cells were placed in 20 ml glass scintillation vials (3 cells *per* vial along with 15 ml of recording solution that was, where indicated, supplemented with vehicle or compound) and incubated at room temperature on a 3-D rotator (Lab Line, Melrose Park, IL). After 20 min, cells were transferred to a recording chamber continuously perfused with the appropriate drug, vehicle or control solution. In some experiments, we recorded isochronal

JPET Fast Forward. Published on April 2, 2013 as DOI: 10.1124/jpet.113.203620
This article has not been copyedited and formatted. The final version may differ from this version.

activation curves before and after incubation in the presence or absence of drug or vehicle. No cell was exposed to more than one drug or vehicle condition.

Channels were activated by hyperpolarizing voltage steps applied in -10 mV decrements for 5 (HCN1), 30 (HCN2) or 60 s (HCN3 and 4). The amplitude of the instantaneous tail currents following each sweep was determined as the difference between the plateau current (observed after the voltage-clamp has settled and the uncompensated linear capacitance decayed but before marked channel closure) and the baseline current (observed after deactivation was complete). These relationships were then fit with a Boltzmann equation (Equation 2) where A_1 is the current offset, A_2 the maximal amplitude, V the test voltage, $V_{1/2}$ the activation mid-point, and s the slope factor.

$$(2) \qquad I(V) = A_1 + A_2/\{1 + e^{(V - V_{1/2})/s}\}$$

Dose-response data were fit using the Hill equation (Equation 3) where R is the response, R_{MAX} the maximal response, [A] the alkylphenol concentration, EC_{50} the ligand concentration that produces a half-maximal response, and *n* the Hill coefficient.

$$(3) \qquad R / R_{max} = 1/\{1 + (EC_{50}/[A])^n\}$$

Fluorescence quench measurement of bilayer modification by di-alkylphenols Large unilamellar vesicles (LUVs), loaded with the disodium salt of the water-soluble fluorophore 8-aminonaphthalene-1,3,6-trisulfonic acid (ANTS), were made of 1,2-dierucoyl-s*n*-glycero-3-phosphocholine ($DC_{22:1}$ PC) using a four-part process of sonication, freeze-thaw cycles,

JPET Fast Forward. Published on April 2, 2013 as DOI: 10.1124/jpet.113.203620
This article has not been copyedited and formatted. The final version may differ from this version.

extrusion, and elution. The LUVs were doped with the naturally occurring mixture of gramicidins (gA) from *B. brevis* (gA:lipid mole ratio ~1:1000) and incubated for 20-24 hours at 12.5 ˚C. The fluorescence produced by ANTS is quenched by thallium (Tl^+). Tl^+ and ANTS cross the bilayer slowly, whereas the bilayer-spanning gA channels are very Tl^+ permeable, such that the Tl^+ influx rate (the rate of fluorescence quenching) becomes a measure of the number of conducting channels in the LUV membranes. To measure the fluorescence quench rate (at 25 °C), the ANTS-loaded LUVs were mixed with the Tl^+ quencher using a stopped-flow spectrofluorometer (Applied Photophysics, SX.20). The fluorescence quench rate was determined at t = 2 ms using Equation 4 wherein τ_0 and β were determined from a fit of the stretched exponential function (Equation 5) to fluorescence recorded between 2 and 100 ms after addition of Tl^+. F_0, F(t) and F∞ represent the fluorescence at time zero, time t and at infinity respectively (Ingólfsson and Andersen, 2010; Ingólfsson et al., 2010). All experiments were done in triplicate, or more.

$$k(t) = (\beta/\tau_0) \cdot (t/\tau_0)^{(\beta-1)} \quad (4)$$

$$F(t) = F_\infty + (F_0\text{-}F_\infty) \cdot e^{-(t/\tau_0)^\beta} \quad (5)$$

Chemicals and reagents NaCl (S7653), KCl (P9333), $MgCl_2$ (M2670), HEPES-free acid (H4034), 2,4-DTBP (137731), 2,6-DTBP (D48400), DHßCD (H107), and *Bacillus brevis* gA (G5002) were from Sigma Aldrich (St. Louis, MO; catalog numbers as indicated). Propofol, 2,4-DSBP (S367907) and 2,6-DSBP (152830050) were from TCI America (Portland, OR), Sigma Rare Chemicals Library and Acros Organics (Pittsburgh PA), respectively. ANTS (A350) was from Invitrogen (Eugene, OR) and $DC_{22:1}$ PC (850398) was from Avanti Polar Lipids (Alabaster,

AL). Stock solutions of alkylphenols were stored at -20 ^{o}C for no more than one week while dilutions in recording solutions were prepared on the day of use. Sterile samples of Diprivan® (1% propofol in intralipid, which contains: 10% soybean oil; 2.25% glycerol; 1.2% egg lecithin; 0.005% EDTA-Na_2 each as W/V) was obtained from Abraxis Bioscience (Schaumburg, IL) and kept at 4 ^{o}C.

Data and statistical analysis Electrophysiological data analysis was performed in PulseFit (HEKA Elektronik) and custom analysis routines written in IgorPro (Wavemetrics Corporation, Lake Oswego, OR). Behavioral data were compiled and analyzed in Excel (Microsoft Corporation, Redmond, WA). Fluorescence quench data were analyzed using custom routines in Matlab (MathWorks, MA) and Origin (OriginLab, MA). Statistical analysis was performed using one-way ANOVA with post hoc Holm-Sidak analysis (enabled in SigmaStat V3.1, Systat Software, Point Richmond, CA). Unless a reference population is defined, tests were performed across all possible pairs and relevant pairs identified from the matrix post hoc. All data are presented as mean ± SEM; for ES_{50}, the error was determined using the Jackknife method. For normalized data, the error around the denominator is that factor's observed error divided by its observed mean.

JPET Fast Forward. Published on April 2, 2013 as DOI: 10.1124/jpet.113.203620
This article has not been copyedited and formatted. The final version may differ from this version.

RESULTS

Subhypnotic doses of propofol reduce mechanical and thermal hyperalgesia Figure 1A shows $P_{W,IPSI}$ and $P_{W,CONTRA}$ in post-PNL mice as a function of stimulus strength (Von Frey fibers ranging from 0.6 to 4 g) and *i.p.* propofol administration (cumulative dose of propofol ranging from 0 to 60 mg/kg). At these doses, propofol markedly reduced the mechanical hyperalgesia in the ipsilateral paw with only modest disturbance of normal mechanical nociceptive response, as monitored in the contralateral paw. $P_{W,IPSI}$ is higher than $P_{W,CONTRA}$ in the absence of propofol, but the difference is significantly reduced upon administration of 20 mg/kg propofol and, at a dose of 60 mg/kg, the response becomes indistinguishable from the control value of $P_{W,CONTRA}$. In contrast, 20 to 60 mg/kg (cumulative dose) propofol had no statistically significant effect on $P_{W,CONTRA}$ suggesting that in the absence of neuropathy, mechanical nociceptive reflexes are relatively insensitive to propofol (consistent with the results of (Udesky et al., 2005)).

In Figure 1B, we plot $P_{W,IPSI}$ and $P_{W,CONTRA}$ as a function of the contralateral control value. In each case the ratios determined across the 2.5 to 4 g stimulus strengths were averaged (see Materials and Methods). Figure 1B shows that subhypnotic propofol provides an ~80% reversal of the neuropathic phenotype (the ratio drops from 3.3 to 1.6, where unity would represent complete amelioration).

Figures 1C and D plot, respectively, the Logit transformation of the data presented in Figure 1A and the extracted 50% stimulus response value (ES_{50}) as a function of cumulative drug dose. These data show that subhypnotic propofol reverses the neuropathic phenotype accompanied by a modest nociceptive analgesia. In the absence of propofol, vehicle injection was without effect; ipsilateral ES_{50} values were 2.4 ± 0.01 and 2.3 ± 0.01 (before and after

JPET Fast Forward. Published on April 2, 2013 as DOI: 10.1124/jpet.113.203620
This article has not been copyedited and formatted. The final version may differ from this version.

vehicle, respectively) whereas contralateral values were 4.8 ± 0.1 and 4.6 ± 0.1. No animals lost their righting reflex consistent with previous demonstrations that >100 mg/kg *i.p.* propofol is required for obviation of this reflex (Lingamaneni et al., 2001; Udesky et al., 2005). We conclude that selective suppression of neuropathic mechanical hyperalgesia occurs at propofol doses that are three- to ten-fold lower than those producing hypnosis.

Figure 2 shows the assessment of thermal hyperalgesia analyzed in a manner equivalent to that shown in Figure 1 for mechanical hyperalgesia. Figure 2A and B plot $HPWL_{IPSI}$ and $HPWL_{CONTRA}$ values at stimulus strengths of 15 and 30%, respectively (each as a function of the cumulative *i.p.* propofol dose) whereas Figures 2C and D show the latencies as a function of the contralateral control value (Figure 2C) and their cognate zero drug condition (Figure 2D). As observed with mechanical hyperalgesia we see that subhypnotic doses of propofol relieve neuropathic thermal hyperalgesia. In the absence of propofol, vehicle injection was without effect; before and after vehicle administration ipsilateral withdrawal was 2.2 and 2.3 (each ± 0.3) times as fast as pre-injection contralateral withdrawal.

2,6 di-tert-butylphenol is a potent antagonist of HCN1 channel gating HCN1 is implicated in the etiology of neuropathic pain and is sensitive to propofol. As there is selectivity among alkylphenols for $GABA_A$-Rs, we explored whether such selectivity was also true for HCN channels.

Figure 3A shows TEVC recordings from *Xenopus* oocytes expressing homomeric HCN1 channels (Left) and the corresponding tail currents (Fig. 3A, Right) obtained following incubation with either DMSO alone (Top) or 10 μM 2,6-DTBP (Bottom). In all four panels, the red line highlights the trace recorded with an activation voltage of -65 mV. Qualitative

JPET Fast Forward. Published on April 2, 2013 as DOI: 10.1124/jpet.113.203620
This article has not been copyedited and formatted. The final version may differ from this version.

inspection of the data suggests that 2,6-DTBP makes HCN1 channels harder to activate or open, maybe both. The compound slows opening, accelerates closing, and shifts gating to more hyperpolarized potentials. The equilibrium activation curves confirm the latter observation (Figure 3B). Such findings are qualitatively identical to the effects of propofol (Cacheaux et al., 2005).

From recordings such as those shown in Figure 3A and B, we constructed a concentration response relationship for the 2,6-DTBP-induced shift in $V_{1/2}$ of HCN1 gating (Fig. 3C Top – data fit by the solid line). These results show that 2,6-DTBP is a five- to six-fold more potent inhibitor of channel gating than propofol (EC_{50} of 2.3 μM versus 13 μM), and that the two compounds have similar maximal efficacy ($V_{1/2}$ of -32 mV versus -45 mV) and apparent stoichiometry (*n* of 1.4 versus 1.1) when the drug effects are determined under equivalent experimental conditions (Lyashchenko et al., 2007). Importantly, 2,6-DTBP had similar efficacy whether it was solubilized in DMSO or DHßCD ($V_{1/2}$ after 20 min incubation with 20 μM 2,6-DTBP was -31.9 mV ± 0.7, n = 6 with DMSO versus -27.7 mV ± 0.7, n = 6 with DHßCD).

To gain insight into whether 2,6-DTBP alters the behavior of fully activated channels, we determined the maximal current density (as obtained from fits of the Boltzmann equation to equilibrium activation curves) before and after incubation in the presence or absence of 2,6-DTBP or vehicle alone. In all cases, the post-incubation current was larger than the pre-incubation current but this run-up appeared to be modestly blunted by 2,6-DTBP (Control: 121% ± 4, n = 8; DHßCD: 124% ± 7, n = 7; 20 μM 2,6-DTBP: 108% ± 7, n = 6; the difference did not reach statistical significance). The run-up in current amplitude may be due to translocation of vesicular channels into the plasma membrane during incubation. In summary, the primary effect

JPET Fast Forward. Published on April 2, 2013 as DOI: 10.1124/jpet.113.203620
This article has not been copyedited and formatted. The final version may differ from this version.

of 2,6-DTBP appears similar to that of propofol, which is to stabilize the closed/deactivated state of HCN1 channels with little effect on the conduction path (Lyashchenko et al., 2007).

The alkylphenol adduct sensitivity of HCN1 channels contraposes that of $GABA_A$ receptors

To examine further the nature of the selective alkylphenol association with HCN1 channels, we asked whether coupling of butylphenols to HCN1 channels displayed any dependence on the structure or location of the alkyl adducts attached to the phenol ring. Specifically, we examined the ability of 2,6-di-*sec*- as well as 2,4-di-*tert*- and 2,4-di-*sec*-butylphenols to inhibit HCN1 channel gating. Figure 3C plots the concentration-response relations for 2,6-DSBP and 2,6-DTBP (Top) and 2,4-DSBP and 2,4-DTBP (Bottom). In each case, the dashed lines through the respective data represent the fit of the Hill equation to the 2,6-DTBP results, offset by two-, 15- and 23-fold (for 2,4-DTBP, 2,6-DSBP and 2,4-DSBP, respectively). There is a strong preference for the tertiary versus the secondary butyl side chains (by more than ten-fold) and a (weaker) preference for 2,6 over 2,4 substitutions (~two-fold). Importantly, the preference for tertiary butyl groups is the inverse of the steric requirements that modulate alkylphenol effects on $GABA_A$-Rs.

As we cannot determine the maximal efficacy of the less potent alkylphenols (at the highest concentrations tested, the aqueous solubility limit is exceeded by visual inspection, see also Supplemental Methods), it is possible HCN1 channels discriminate between di-*sec* and di-*tert* butylphenols more fully than is suggested by comparison of potency alone (Figure 3).

2,6 di-tert-butylphenol selectively antagonizes gating of HCN1 Propofol is an efficacious, potent antagonist of HCN1 channel gating with marked selectivity for HCN1 over the other HCN

JPET Fast Forward. Published on April 2, 2013 as DOI: 10.1124/jpet.113.203620
This article has not been copyedited and formatted. The final version may differ from this version.

isoforms; 20 μM propofol shifts $V_{1/2}$ by -45 mV for HCN1 but only -9 mV and 0 mV for HCN2 and 4, respectively (Lyashchenko et al., 2007), and -0.6 mV ± 0.1 (n = 6) for HCN3 (data not shown). Figure 3D shows that 2,6-DTBP retains this selectivity profile, suggesting that 2,6-DTBP could be an analgesic with minimal hypnotic effect.

2,6-di-tert-butylphenol reverses the neuropathic responses to mechanical and thermal insults while leaving nociception largely intact 2,6-DTBP does not potentiate $GABA_A$-Rs nor is it a general anesthetic at concentrations equivalent to those that are hypnotic for propofol (James and Glen, 1980; Krasowski et al., 2001); and references in Table 1). Thus, if potentiation of $GABA_A$-Rs represents a critical aspect of propofol's efficacy as a neuropathic pain-selective analgesic, then 2,6-DTBP would be expected to be ineffective. In contrast, if HCN1-containing I_H channels were involved in propofol's neuropathic analgesic activity we would anticipate 2,6-DTBP would retain a propofol-like efficacy (see Discussion for possible alternative targets). Figures 4 and 5 show that 2,6-DTBP ameliorates the behavioral consequences of PNL-induced hyperalgesia with respect to both mechanical (Fig. 4) and thermal insults (Fig. 5) and does so with a preferential retention of nociceptive transmission, a finding that closely mirrors the activity seen with sub-hypnotic propofol. These therapeutic effects are not due to vehicle. In the absence of 2,6-DTBP, ipsilateral ES_{50} values were 1.5 g ± 0.1 and 1.3 g ± 0.3 before and after vehicle whereas contralateral values were 3.7 g ± 0.2 and 4.2 g ± 0.6; similarly, before and after vehicle administration the ipsilateral withdrawal was 1.8 ± 0.2 and 1.6 ± 0.1 times as fast as preinjection contralateral withdrawal.

JPET Fast Forward. Published on April 2, 2013 as DOI: 10.1124/jpet.113.203620
This article has not been copyedited and formatted. The final version may differ from this version.

Alkylphenol inhibition of HCN1 channels is not due to effects on the lipid bilayer The alkylphenols are hydrophobic, with calculated octanol/water partition coefficients (expressed as cLog P) of ~5 (Krasowski et al., 2001), comparable to that of potent bilayer modifiers (Rusinova et al., 2011). General anesthetics have been shown to exert many, but perhaps not all, of their effects *via* specific interactions with ion channels (Eger et al., 2008), thereby leaving open the possibility that those that are lipophiles (such as the alkylphenols) may also alter embedded membrane protein function *via* interactions with the lipid bilayer ((Lundbaek et al., 2010), cf. Figure 6A). We therefore tested whether the alkylphenols alter bilayer properties at the concentrations where they alter HCN channel function. To do so, we examined the ability of propofol and the butylphenols to alter the energetics of gA channel formation (Figure 6B) using a gA-based fluorescence assay (Ingólfsson and Andersen, 2010; Ingólfsson et al., 2010; Lundbaek et al., 2010).

Figure 6C and D show the effect of 2,6-DTBP on the time course of Tl^+-induced quenching of the fluorescence emission of ANT encapsulated into gA-doped LUVs. Because Tl^+ primarily enters the LUV through membrane-spanning gA channels, changes in the fluorescence quench rate reflect changes in the average number of channels/vesicle. Addition of increasing concentrations of 2,6-DTBP had only a weak effect on either the rate or extent of quenching, meaning that alkylphenols have little effect on the gramicidin monomer↔dimer equilibrium (which varies with changes in lipid bilayer physical properties); this is especially evident when the data here are contrasted with those obtained in vesicles doped with a potent membrane modifying amphiphile, capsaicin (see Supplemental Results; Figure S5).

A modest effect on the quench rate is also observed when vesicles are doped with the other butylphenols but not with propofol (Figure 6E). Importantly, there is no correspondence

between the rank order of potencies by which the five alkylphenols inhibit HCN1 gating (Figure 6F) and their modest effects on membrane deformation energetics (Figure 6E).

One caveat with directly comparing the EC_{50} of channel inhibition with the effect of the alkylphenols on the gA-mediated fluorescence quench rate is the question of the meaning of the added aqueous concentration. Partitioning of compounds with a high cLog P will tend to lower the added aqueous concentration even when the aqueous phase is present in what would normally be considered vast excess. However, the effective lipid:aqueous volumes of our oocyte incubations and our vesicle incubations are similar indicating that while the aqueous phase 'free' concentration of the alkylphenols will be lowered (by ~10-fold over the added initial aqueous concentration), this will be similar in the two assays. We conclude that neither 2,6-DTBP nor propofol alter HCN1 channel function through changes in lipid bilayer properties at the concentrations tested, an observation that supports the notion that alkylphenols interact specifically and selectively with HCN1.

JPET Fast Forward. Published on April 2, 2013 as DOI: 10.1124/jpet.113.203620
This article has not been copyedited and formatted. The final version may differ from this version.

DISCUSSION

We tested the hypothesis that I_H pacemaker channel antagonists with selectivity for the HCN1 subunit would provide analgesia in a murine model of neuropathic pain, and found that two closely related alkylphenols, the intravenous anesthetic propofol and its non-anesthetic congener, 2,6-DTBP, both inhibit heterologously expressed HCN1 channels and are antihyperalgesic in a mouse model of neuropathic pain. Our results are consistent with selective inhibition of HCN1 channels being the presumptive antihyperalgesic mechanism for this class of compounds. This supposition is supported by data demonstrating that the structurally related clove extract, eugenol (2-methoxy-4-(2-propenyl)phenol), inhibits I_H in trigeminal neurons and reverses mechanical allodynia following chronic nerve constriction (Yeon et al., 2011). Recently, 2-ethoxy-N-((1-(4-isopropylpiperazin-1-yl)cyclohexyl)methyl)benzamide, a 1,1-disubstituted cyclohexane which appears to selectively inhibit HCN1 channels, has been shown to alleviate nerve injury-induced tactile allodynia in a murine model (McClure et al., 2011), further supporting the idea that specific HCN1 channel blockade might have therapeutic potential in the treatment of neuropathic pain.

Antihyperalgesic action of anesthetic and non-anesthetic alkylphenols Here, we demonstrate that propofol, at subhypnotic doses, (Figures 1 and 2) and 2,6-DTBP (Figures 4 and 5) profoundly reduce hyperalgesia in a mouse model of neuropathic pain. These observations are consistent with prior results demonstrating that propofol has extended analgesic properties. For example, human subjects who received propofol anesthesia for elective surgical procedures reported less postoperative pain than those anesthetized with the volatile general anesthetics isoflurane (Cheng et al., 2008) or sevoflurane (Tan et al., 2010). In humans, subanesthetic doses

of propofol (*i.e.* 10 to 25% of the dose required to produce general anesthesia) are associated with a decrease in tibial pressure-induced pain (Briggs et al., 1982), while concentrations sufficient to produce mild to moderate sedation are analgesic with respect to acute thermal pain ((Frölich et al., 2005) and see also (Anker-Møller et al., 1991). With respect to pathologic pain, and therefore of direct relevance to the present study, intrathecally administered propofol dose-dependently suppresses algesic behavior (paw flinching and shaking) elicited by subcutaneous injection of formalin into the hindpaw in rats (Nishiyama et al., 2004). Additionally, subcutaneous injection of propofol suppresses bee venom-induced algesic behaviors in rats when administered ipsilateral, but not contralateral, to the site of venom injection (Sun et al., 2005), suggesting a peripheral, rather than central, site of action.

Potential sites of analgesic action of anesthetic and non-anesthetic alkylphenols During general anesthesia, the steady-state plasma concentration of free propofol is on the order of 1 μM (Table 1). Inhibition of neuropathic pain emerges at three- to ten-fold lower doses than the ED_{50} for anesthesia (Erenmemisoglu et al., 1993; Lingamaneni et al., 2001), or 0.1 to 0.3 μM. If propofol and 2,6-DTBP partition similarly and proportionally, we further estimate that an analgesic dose of 2,6-DTBP of 80 mg/kg (*i.p.*) would yield a predicted free serum concentration of ~0.6 μM. Based on dose-response relations determined from heterologously expressed channels (Figure 3), such a 2,6-DTBP concentration is anticipated to have a marked effect on HCN1 channel gating whereas that of propofol is on the cusp of the effective dose - though estimates of alkylphenol potency based on inhibition of heterologously expressed channels can be an underestimate by a factor of ~10 due to the consequences of partitioning into the lipophilic interior of *Xenopus* oocytes (see Results and also (Cacheaux et al., 2005)). Together, our

JPET Fast Forward. Published on April 2, 2013 as DOI: 10.1124/jpet.113.203620
This article has not been copyedited and formatted. The final version may differ from this version.

results are consistent with the alkylphenols exerting their antihyperalgesic action *via* association with, and inhibition of, HCN1-containing, peripheral I_H channels. Given a partial sensitivity of HCN2 to both propofol and 2,6-DTBP, a synergistic contribution of HCN2 inhibition (Ying et al., 2006; Emery et al., 2011) cannot be discounted. A more critical examination of this question will require analysis of analgesia in mice lacking alkylphenol-sensitive HCN isoforms.

If alkylphenols are not exerting their analgesic actions *via* HCN channels, what are plausible alternative targets? The key molecular targets of propofol-induced hypnosis are the $GABA_A$-Rs (Franks, 2008). However, $GABA_A$-Rs are unlikely to mediate the neuropathic analgesic action of alkylphenols as heterologously expressed ($\alpha_1\beta_2\gamma_{2s}$ subunits (Krasowski et al., 2001; Ahrens et al., 2009)) and native (*Xenopus laevis* spinal cord neurons (Krasowski et al., 2001)) $GABA_A$-Rs are insensitive to 2,6-DTBP. As for glycine receptors (Gly-Rs), while inhibition of spinal Gly-Rs produces allodynia (Sherman and Loomis, 1994), and both propofol (Pistis et al., 1997; Ahrens et al., 2004) and 2,6-DTBP (Ahrens et al., 2004) enhance the gating of heterologously expressed Gly-Rs, their sensitivity is too low for them to be relevant targets in this regard.

Among voltage-gated channels, $Na_V1.3$, 1.7, 1.8 and 1.9 are implicated as mediators of inflammatory and neuropathic pain (Jarvis et al., 2007; Costigan et al., 2009; Dib-Hajj et al., 2009). Although the alkylphenol sensitivity of these isoforms has not been examined in detail, the Na^+ currents of neurohypophysial nerve terminals are inhibited by micromolar concentrations of propofol (Ouyang et al., 2003) and at least one isoform ($Na_V1.2$) is inhibited by 2,6-DTBP albeit at relatively high concentrations (> 10 μM) (Haeseler and Leuwer, 2003). Interestingly, an extensive library screen by Abbott laboratories and Icagen identified a 4-substituted 2,6-dimethoxyphenyl as a Na_V antagonist with preference for $Na_V1.8$ (Jarvis et al., 2007). This

JPET Fast Forward. Published on April 2, 2013 as DOI: 10.1124/jpet.113.203620
This article has not been copyedited and formatted. The final version may differ from this version.

compound ameliorates some modalities of neuropathic pain at doses comparable to those we show to be efficacious for 2,6-DTBP. Finally, we note that 2,6-DTBP is a presumptive inhibitor of key enzymes in the arachidonic acid cascade (*e.g.*, (Song et al., 1999)). It is unlikely the anti-hyperalgesic activity of alkylphenols is related to cyclooxygenase inhibition (given that efficacy as an inhibitor of these enzymes is a poor predictor of a compound's efficacy against neuropathic pain (Vo et al., 2009)), but it suggests that alkylphenol anti-hyperalgesic activity may result from a combination of actions with HCN1 inhibition being a major contributor.

The CSF concentration of propofol required for anesthesia is approximately one-sixth of that in plasma (Table 1). Examination of the extent to which 2,6-DTBP shares this property and exploitation of relative CSF sparing would benefit development of alkylphenols with respect to specifically targeting peripheral sensitization.

Mechanistic basis for selective inhibition of HCN1 channels by di-propyl and di-butyl alkylphenols We have previously shown that propofol modifies gating of HCN channels in the closed-resting and closed-activated states with little or no pore-blocking effect (Lyashchenko et al., 2007). We now demonstrate that the HCN1 sensitivity to alkylphenols displays a dependence on the steric arrangement of the alkyl adducts. With regard to $GABA_A$-R potentiation, such a steric effect has previously been interpreted as evidence for the existence of a protein pocket of circumscribed dimensions within the channel (Franks and Lieb, 1985; Krasowski et al., 2001). Such phenomena can, however, also arise in a system in which no binding site exists (Ingólfsson and Andersen, 2011), and we examined the ability of alkylphenols to alter lipid bilayer properties. Whereas the butylphenols (but not propofol) modestly altered lipid bilayer properties (as sensed by a membrane-spanning channel), this was seen only at

JPET Fast Forward. Published on April 2, 2013 as DOI: 10.1124/jpet.113.203620
This article has not been copyedited and formatted. The final version may differ from this version.

concentrations much higher than those where they altered HCN1 channel function - and there was no apparent rank order in their effect on bilayer properties, and certainly not one that corresponded to the clear rank order effect with respect to inhibition of HCN1 (Figure 6E versus F). Propofol has recently been shown to occupy a defined pocket in a $GABA_A$-R homolog (Nury et al., 2011); consequently, we hypothesize that a similar site exists within HCN1 albeit with mirror-image dependence (as compared to the $GABA_A$-R) on the steric arrangement of the alkylphenol.

Alkylphenol effects on lipid membranes Interestingly, while their effect on the energetics of gA channel formation was modest, the trend was for di-butylphenols to reduce the fluorescence quench rate, meaning that they shifted the gA monomer↔dimer equilibrium toward the non-conducting monomers. The usual result is that small bilayer-active molecules shift the monomer↔dimer equilibrium toward the conducting dimers (*e.g.*, capsaicin – see Figure S5 and also (Lundbaek et al., 2010)) though there are exceptions such as the long-chain alcohols (Ingólfsson and Andersen, 2011). The parsimonious interpretation is that the di-butyl-phenols increase acyl chain order and bilayer thickness, though we do not understand why.

Conclusions We have shown that the closely related anesthetic and non-anesthetic alkylphenols, propofol and 2,6-DTBP, selectively inhibit HCN1 pacemaker channels and provide selective reversal of mechanical and thermal hyperalgesia resulting from peripheral nerve injury in a mouse model. Although these findings do not establish that alkylphenols exert their analgesic action *via* HCN1 channel inhibition *in vivo*, they establish that 2,6-DTBP (or derivatives thereof) represent a novel class of analgesic agents that might selectively target

chronic neuropathic pain. Our observations also provide a chemical lead for development of peripherally restricted HCN1-selective antagonists based on a widely used, and safe, therapeutic agent. It is interesting to speculate that a suppression of peripheral hyperexcitability by propofol accounts for the lower post-surgical pain that has been reported when it is used to provide anesthesia.

ACKNOWLEDGEMENTS We thank Juliane Stieber and Andreas Ludwig for kindly providing us with the human HCN3 clone, Steven Siegelbaum's laboratory for providing us with *Xenopus* oocytes, Dr. Charles Inturissi for his thoughtful comments, and Dr. Kane Pryor for providing the estimated propofol concentrations in Footnote A to Table 1.

AUTHOR CONTRIBUTIONS

Participated in research design: Andersen, Flood, Hemmings, Tibbs.

Conducted experiments: Herold, Rowley, Sanford, Tibbs.

Performed data analysis: Goldstein, Herold, Proekt, Sanford, Tibbs.

Wrote or contributed to the writing of the manuscript: Andersen, Flood, Goldstein, Hemmings, Tibbs.

CONFLICT OF INTEREST GRT, PAG and PDF have applied for a patent to exploit alkylphenols in the treatment of neuropathic pain. None of these authors or any of the coauthors have any other financial interest in this work.

REFERENCES

Ahrens J, Haeseler G, Leuwer M, Mohammadi B, Krampfl K, Dengler R and Bufler J (2004) 2,6 di-*tert*-butylphenol, a nonanesthetic propofol analog, modulates α1β glycine receptor function in a manner distinct from propofol. *Anesth Analg* **99**:91-96.

Ahrens J, Leuwer M, de la Roche J, Foadi N, Krampfl K and Haeseler G (2009) The non-anaesthetic propofol analogue 2,6-di-*tert*-butylphenol fails to modulate $GABA_A$ receptor function. *Pharmacology* **83**:95-98.

Andersen OS (2008) Perspectives on how to drug an ion channel. *J Gen Physiol* **131**:395-397.

Anker-Møller E, Spangsberg N, Arendt-Nielsen L, Schultz P, Kristensen MS and Bjerring P (1991) Subhypnotic doses of thiopentone and propofol cause analgesia to experimentally induced acute pain. *Br J Anaesth* **66**:185-188.

Briggs LP, Dundee JW, Bahar M and Clarke RS (1982) Comparison of the effect of diisopropyl phenol (ICI 35, 868) and thiopentone on response to somatic pain. *Br J Anaesth* **54**:307-311.

Cacheaux LP, Topf N, Tibbs GR, Schaefer UR, Levi R, Harrison NL, Abbott GW and Goldstein PA (2005) Impairment of hyperpolarization-activated, cyclic nucleotide-gated channel function by the intravenous general anesthetic propofol. *J Pharmacol Exp Ther* **315**:517-525.

Chaplan SR, Guo HQ, Lee DH, Luo L, Liu C, Kuei C, Velumian AA, Butler MP, Brown SM and Dubin AE (2003) Neuronal hyperpolarization-activated pacemaker channels drive neuropathic pain. *J Neurosci* **23**:1169-1178.

Chen X, Shu S and Bayliss DA (2005) Suppression of I_h contributes to propofol-induced inhibition of mouse cortical pyramidal neurons. *J Neurophysiol* **94**:3872-3883.

Cheng SS, Yeh J and Flood P (2008) Anesthesia matters: patients anesthetized with propofol have less postoperative pain than those anesthetized with isoflurane. *Anesth Analg* **106**:264-269.

Costigan M, Scholz J and Woolf CJ (2009) Neuropathic pain: a maladaptive response of the nervous system to damage. *Annu Rev Neurosci* **32**:1-32.

Dawidowicz AL, Fijalkowska A, Nestorowicz A, Kalitynski R and Trojanowski T (2003) Cerebrospinal fluid and blood propofol concentration during total intravenous anaesthesia for neurosurgery. *Br J Anaesth* **90**:84-86.

Dawidowicz AL and Kalitynski R (2003) HPLC investigation of free and bound propofol in human plasma and cerebrospinal fluid. *Biomed Chromatogr* **17**:447-452.

Dawidowicz AL, Kalitynski R, Nestorowicz A and Fijalkowska A (2002) Changes of propofol concentration in cerebrospinal fluid during continuous infusion. *Anesth Analg* **95**:1282-1284.

Dib-Hajj SD, Black JA and Waxman SG (2009) Voltage-gated sodium channels: therapeutic targets for pain. *Pain Med* **10**:1260-1269.

Dray A (2008) Neuropathic pain: emerging treatments. *Br J Anaesth* **101**:48-58.

Eger EI, 2nd, Tang M, Liao M, Laster MJ, Solt K, Flood P, Jenkins A, Raines D, Hendrickx JF, Shafer SL, Yasumasa T and Sonner JM (2008) Inhaled anesthetics do not combine to produce synergistic effects regarding minimum alveolar anesthetic concentration in rats. *Anesth Analg* **107**:479-485.

Emery EC, Young GT, Berrocoso EM, Chen L and McNaughton PA (2011) HCN2 ion channels play a central role in inflammatory and neuropathic pain. *Science* **333**:1462-1466.

Emery EC, Young GT and McNaughton PA (2012) HCN2 ion channels: an emerging role as the pacemakers of pain. *Trends Pharmacol Sci* **33**:456-463.

Engdahl O, Abrahams M, Bjornsson A, Vegfors M, Norlander B, Ahlner J and Eintrei C (1998) Cerebrospinal fluid concentrations of propofol during anaesthesia in humans. *Br J Anaesth* **81**:957-959.

Erenmemisoglu A, Madenoglu H and Teko Y (1993) Antinociceptive effect of propofol on somatic and visceral pain in subhynotic doses. *Curr Ther Res* **53**:677-681.

Franks NP (2008) General anaesthesia: from molecular targets to neuronal pathways of sleep and arousal. *Nat Rev Neurosci* **9**:370-386.

Franks NP and Lieb WR (1985) Mapping of general anaesthetic target sites provides a molecular basis for cutoff effects. *Nature* **316**:349-351.

Frölich MA, Price DD, Robinson ME, Shuster JJ, Theriaque DW and Heft MW (2005) The effect of propofol on thermal pain perception. *Anesth Analg* **100**:481-486.

Haeseler G and Leuwer M (2003) High-affinity block of voltage-operated rat IIA neuronal sodium channels by 2,6 di-*tert*-butylphenol, a propofol analogue. *Eur J Anaesthesiol* **20**:220-224.

Ingólfsson HI and Andersen OS (2010) Screening for small molecules' bilayer-modifying potential using a gramicidin-based fluorescence assay. *Assay Drug Develop Technol* **8**:427-436.

Ingólfsson HI and Andersen OS (2011) Alcohol's effects on lipid bilayer properties. *Biophys J* **101**:847-855.

Ingólfsson HI, Sanford RL, Kapoor R and Andersen OS (2010) Gramicidin-based fluorescence assay; for determining small molecules potential for modifying lipid bilayer properties. *J Vis Exp, Epub Date* - 2010/10/26, DOI: 10.3791/2131.

James R and Glen JB (1980) Synthesis, biological evaluation, and preliminary structure-activity considerations of a series of alkylphenols as intravenous anesthetic agents. *J Med Chem* **23**:1350-1357.

Jarvis MF, Honore P, Shieh CC, Chapman M, Joshi S, Zhang XF, Kort M, Carroll W, Marron B, Atkinson R, Thomas J, Liu D, Krambis M, Liu Y, McGaraughty S, Chu K, Roeloffs R, Zhong C, Mikusa JP, Hernandez G, Gauvin D, Wade C, Zhu C, Pai M, Scanio M, Shi L, Drizin I, Gregg R, Matulenko M, Hakeem A, Gross M, Johnson M, Marsh K, Wagoner PK, Sullivan JP, Faltynek CR and Krafte DS (2007) A-803467, a potent and selective Nav1.8 sodium channel blocker, attenuates neuropathic and inflammatory pain in the rat. *Proc Natl Acad Sci U S A* **104**:8520-8525.

Jensen TS, Madsen CS and Finnerup NB (2009) Pharmacology and treatment of neuropathic pains. *Curr Opin Neurol* **22**:467-474.

Jiang YQ, Xing GG, Wang SL, Tu HY, Chi YN, Li J, Liu FY, Han JS and Wan Y (2008) Axonal accumulation of hyperpolarization-activated cyclic nucleotide-gated cation channels contributes to mechanical allodynia after peripheral nerve injury in rat. *Pain* **137**:495-506.

Kouranova EV, Strassle BW, Ring RH, Bowlby MR and Vasilyev DV (2008) Hyperpolarization-activated cyclic nucleotide-gated channel mRNA and protein expression in large versus small diameter dorsal root ganglion neurons: Correlation with hyperpolarization-activated current gating. *Neuroscience* **153**:1008-1019.

Krasowski MD, Jenkins A, Flood P, Kung AY, Hopfinger AJ and Harrison NL (2001) General anesthetic potencies of a series of propofol analogs correlate with potency for potentiation of γ-aminobutyric acid (GABA) current at the $GABA_A$ receptor but not with lipid solubility. *J Pharmacol Exp Ther* **297**:338-351.

Lee DH, Chang L, Sorkin LS and Chaplan SR (2005) Hyperpolarization-activated, cation-nonselective, cyclic nucleotide-modulated channel blockade alleviates mechanical allodynia and suppresses ectopic discharge in spinal nerve ligated rats. *J Pain* **6**:417-424.

Lingamaneni R, Krasowski MD, Jenkins A, Truong T, Giunta AL, Blackbeer J, MacIver MB, Harrison NL and Hemmings HC, Jr. (2001) Anesthetic properties of 4-iodopropofol: implications for mechanisms of anesthesia. *Anesthesiology* **94**:1050-1057.

Lundbaek JA, Collingwood SA, Ingolfsson HI, Kapoor R and Andersen OS (2010) Lipid bilayer regulation of membrane protein function: gramicidin channels as molecular force probes. *J Royal Society Interface* **7**:373-395.

Lyashchenko AK, Redd KJ, Yang J and Tibbs GR (2007) Propofol inhibits HCN1 pacemaker channels by selective association with the closed states of the membrane embedded channel core. *J Physiol* **583**:37-56.

Mayer ML and Westbrook GL (1983) A voltage-clamp analysis of inward (anomalous) rectification in mouse spinal sensory ganglion neurones. *J Physiol* **340**:19-45.

McClure KJ, Maher M, Wu N, Chaplan SR, Eckert WA, III, Lee DH, Wickenden AD, Hermann M, Allison B, Hawryluk N, Breitenbucher JG and Grice CA (2011) Discovery of a novel series of selective HCN1 blockers. *Bioorg Med Chem Lett* **21**:5197-5201.

Momin A, Cadiou H, Mason A and McNaughton PA (2008) Role of the hyperpolarization-activated current I_h in somatosensory neurons. *J Physiol* **586**:5911-5929.

Nishiyama T, Matsukawa T and Hanaoka K (2004) Intrathecal propofol has analgesic effects on inflammation-induced pain in rats. *Can J Anaesth* **51**:899-904.

Nury H, Van Renterghem C, Weng Y, Tran A, Baaden M, Dufresne V, Changeux JP, Sonner JM, Delarue M and Corringer PJ (2011) X-ray structures of general anaesthetics bound to a pentameric ligand-gated ion channel. *Nature* **469**:428-431.

Orio P, Madrid R, de la Pena E, Parra A, Meseguer V, Bayliss DA, Belmonte C and Viana F (2009) Characteristics and physiological role of hyperpolarization activated currents in mouse cold thermoreceptors. *J Physiol* **587**:1961-1976.

Ouyang W, Wang G and Hemmings HC, Jr. (2003) Isoflurane and propofol inhibit voltage-gated sodium channels in isolated rat neurohypophysial nerve terminals. *Mol Pharmacol* **64**:373-381.

Pistis M, Belelli D, Peters JA and Lambert JJ (1997) The interaction of general anaesthetics with recombinant $GABA_A$ and glycine receptors expressed in *Xenopus laevis* oocytes: a comparative study. *Br J Pharmacol* **122**:1707-1719.

Rusinova R, Herold KF, Sanford RL, Greathouse DV, Hemmings HC, Jr. and Andersen OS (2011) Thiazolidinedione insulin sensitizers alter lipid bilayer properties and voltage-dependent sodium channel function: implications for drug discovery. *J Gen Physiol* **138**:249-270.

Seltzer Z, Dubner R and Shir Y (1990) A novel behavioral model of neuropathic pain disorders produced in rats by partial sciatic nerve injury. *Pain* **43**:205-218.

Servin F, Desmonts JM, Haberer JP, Cockshott ID, Plummer GF and Farinotti R (1988) Pharmacokinetics and protein binding of propofol in patients with cirrhosis. *Anesthesiology* **69**:887-891.

Sherman SE and Loomis CW (1994) Morphine insensitive allodynia is produced by intrathecal strychnine in the lightly anesthetized rat. *Pain* **56**:17-29.

Smith C, McEwan AI, Jhaveri R, Wilkinson M, Goodman D, Smith LR, Canada AT and Glass PS (1994) The interaction of fentanyl on the Cp_{50} of propofol for loss of consciousness and skin incision. *Anesthesiology* **81**:820-828.

Song Y, Connor DT, Doubleday R, Sorenson RJ, Sercel AD, Unangst PC, Roth BD, Gilbertsen RB, Chan K, Schrier DJ, Guglietta A, Bornemeier DA and Dyer RD (1999) Synthesis, structure-activity relationships, and in vivo evaluations of substituted di-tert-butylphenols as a novel class of potent, selective, and orally active cyclooxygenase-2 inhibitors. 1. Thiazolone and oxazolone series. *J Med Chem* **42**:1151-1160.

Sun YY, Li KC and Chen J (2005) Evidence for peripherally antinociceptive action of propofol in rats: behavioral and spinal neuronal responses to subcutaneous bee venom. *Brain Res* **1043**:231-235.

Tan T, Bhinder R, Carey M and Briggs L (2010) Day-surgery patients anesthetized with propofol have less postoperative pain than those anesthetized with sevoflurane. *Anesth Analg* **111**:83-85.

Tu H, Deng L, Sun Q, Yao L, Han JS and Wan Y (2004) Hyperpolarization-activated, cyclic nucleotide-gated cation channels: roles in the differential electrophysiological properties of rat primary afferent neurons. *J Neurosci Res* **76**:713-722.

Udesky JO, Spence NZ, Achiel R, Lee C and Flood P (2005) The role of nicotinic inhibition in ketamine-induced behavior. *Anesth Analg* **101**:407-411.

Vo T, Rice AS and Dworkin RH (2009) Non-steroidal anti-inflammatory drugs for neuropathic pain: how do we explain continued widespread use? *Pain* **143**:169-171.

Yao H, Donnelly DF, Ma C and LaMotte RH (2003) Upregulation of the hyperpolarization-activated cation current after chronic compression of the dorsal root ganglion. *J Neurosci* **23**:2069-2074.

Yeon KY, Chung G, Kim YH, Hwang JH, Davies AJ, Park MK, Ahn DK, Kim JS, Jung SJ and Oh SB (2011) Eugenol reverses mechanical allodynia after peripheral nerve injury by inhibiting hyperpolarization-activated cyclic nucleotide-gated (HCN) channels. *Pain* **152**:2108-2116.

Ying SW, Abbas SY, Harrison NL and Goldstein PA (2006) Propofol block of I_h contributes to the suppression of neuronal excitability and rhythmic burst firing in thalamocortical neurons. *Eur J Neurosci* **23**:465-480.

FOOTNOTE This work was supported in part by the National Institutes of Health Institute of General Medical Sciences [Grants GM021342, GM021342-35S1, GM58055] and by the Departments of Anesthesiology of Columbia University and Weill Cornell Medical College.

Present Addresses: Department of Anesthesiology, Weill Cornell Medical College, New York, NY 10065 (GRT); Department of Anesthesiology, University of California – San Francisco, San Francisco, CA (PDF)

JPET Fast Forward. Published on April 2, 2013 as DOI: 10.1124/jpet.113.203620
This article has not been copyedited and formatted. The final version may differ from this version.

FIGURE LEGENDS

Figure 1. **Subhypnotic doses of propofol selectively suppress PNL-induced mechanical hyperalgesia with respect to mechanical nociception.**

A, B. $P_{W,IPSI}$ and $P_{W,CONTRA}$ as a function of stimulus fiber strength determined before and after *i.p.* propofol (**A**) and $P_{W,IPSI}$ and $P_{W,CONTRA}$ as a function of $P_{W,CONTRA}$ before drug injection (**B**). Asterisks and crosses indicate P_W values statistically different from control $P_{W,IPSI}$ and $P_{W,CONTRA}$, respectively. In **A** tests are performed separately for each stimulus intensity; in **B** tests are with respect to $P_{W,CONTRA}$.

C, D. Logit transformation of $P_{W,IPSI}$ and $P_{W,CONTRA}$ in the absence or presence of propofol (**C**) and the extracted ES_{50} plotted as a function of drug dose (**D**). In **C**, the color gradations have the same meaning with respect to dose as in **A**, the dashed horizontal line is at a P_W of 0.1. In **D**, asterisks and crosses have the same meaning as in **A** while the lines are linear regressions with R^2 values of 0.98 for the ipsilateral data and 0.99 for the contralateral data; P for both regressions was ≤ 0.01. Data are from 15 mice (except for 0.6 g stimulus, which was for 11 mice).

Figure 2. **Subhypnotic doses of propofol selectively ameliorate PNL-induced thermal hyperalgesia with respect to thermal nociception**.

A, B. HPWL as a function of heat source intensity determined before and after *i.p.* propofol.

C. $HPWL_{IPSI}$ and $HPWL_{CONTRA}$ as a function of $HPWL_{CONTRA}$ before drug injection.

D. $HPWL_{IPSI}$ and $HPWL_{CONTRA}$ as a function of HPWL observed in the cognate paw before drug injection.

JPET Fast Forward. Published on April 2, 2013 as DOI: 10.1124/jpet.113.203620
This article has not been copyedited and formatted. The final version may differ from this version.

Asterisks and crosses indicate HPWL values statistically different from control $HPWL_{IPSI}$ and control $HPWL_{CONTRA}$, respectively. In **C** statistical tests are with respect to $P_{W,CONTRA}$; in **D** tests are within paw only. Data are from 10 (30%) or 14 (15%) mice.

Figure 3. **2,4 and 2,6 tertiary butyl substituted phenols – High potency HCN1 selective pacemaker channel antagonists**.

A. HCN1 TEVC records (Left) and tail currents (Right) obtained following 20 min incubation in either DMSO (Top in gray) or 10 µM 2,6-DTBP (Bottom in black). Red lines highlight records obtained upon activation at -65 mV. Records are from two separate cells but are from the same donor frog and were acquired on the same day.

B. Tail current activation curves for cells shown in **A**. Fits of the Boltzmann function (superimposed lines) yielded values of the $V_{1/2}$ and slope of –60.6 and 8.7 mV (mean –64.8 mV ± 1.9 and 7.5 mV ± 0.3; n = 14) versus –90.8 and 9.7 mV (mean –88.3 mV ± 1.4 and 9.6 mV ± 0.1; n = 6) in the presence of DMSO and 10 µM 2,6-DTBP, respectively.

C. Shift in $V_{1/2}$ of HCN1 gating as a function of the concentrations of 2,6- (Upper panel) or 2,4- (Lower panel) dibutylphenols. The solid line (and indicated parameter values) is from a fit of the Hill function to the 2,6-DTBP concentration response relationship. The dashed lines are the 2,6-DTBP fit line offset by 2, 15 and 23-fold for 2,4-DTBP, 2,6-DSBP and 2,4-DSBP, respectively. As the $V_{1/2}$ elicited by 20 µM 2,6-DTBP was similar irrespective of whether the compound was solubilized in DMSO or DHßCD (see text), these values were pooled here. For DTBPs the shift in $V_{1/2}$ was significant at 1 µM and higher but for DSBPs significance was only observed at 20 µM.

D. Shift in $V_{1/2}$ of gating of HCN1-4 as a function of the indicated concentration of 2,6-DTBP. Asterisks indicate responses statistically different from the paired control.

Figure 4. **2,6-DTBP selectively suppresses PNL-induced mechanical hyperalgesia with respect to mechanical nociception**.

A, B. $P_{W,IPSI}$ and $P_{W,CONTRA}$ as a function of stimulus fiber strength determined before and after *i.p.* 2,6-DTBP (**A**) and $P_{W,IPSI}$ and $P_{W,CONTRA}$ as a function of $P_{W,CONTRA}$ before drug injection (**B**). Asterisks and crosses have the same meaning as in Figure 1.

C, D. Logit transformation of $P_{W,IPSI}$ and $P_{W,CONTRA}$ in the absence or presence of 2,6-DTBP (**C**) and the extracted ES_{50} plotted as a function of drug dose (**D**). In **C**, the color gradations have the same meaning with respect to dose as in **A**, the dashed horizontal line is at a P_W of 0.1. In **D**, asterisks and crosses have the same meaning as in **A** while the lines are linear regressions with R^2 values of 0.91 for the ipsilateral data and 0.92 for the contralateral data; P for both regressions was ≤ 0.05. Data are from 10 mice.

Figure 5. **2,6-DTBP selectively ameliorates PNL-induced thermal hyperalgesia with respect to thermal nociception**.

A, **B**. HPWL as a function of heat source intensity determined before and after *i.p.* 2,6-DTBP.

C. $HPWL_{IPSI}$ and $HPWL_{CONTRA}$ as a function of $HPWL_{CONTRA}$ before drug injection.

D. $HPWL_{IPSI}$ and $HPWL_{CONTRA}$ as a function of HPWL observed in the cognate paw before drug injection.

Asterisks and crosses have the same meaning as in Figure 2. Data are from 10 mice.

JPET Fast Forward. Published on April 2, 2013 as DOI: 10.1124/jpet.113.203620
This article has not been copyedited and formatted. The final version may differ from this version.

Figure 6. Alkylphenol inhibition of HCN1 channels is not accompanied by effects on the lipid bilayer.

A. Mechanisms by which drugs can inhibit membrane protein (ion channel) function: 1) Occluding the pore to block ion movement; 2) binding to sites formed by the channel, to alter function by altering the free energy difference between different channel conformations; 3) binding to selective sites at the channel/bilayer interface, which may alter also the bilayer deformation energy contribution to the free energy difference between different conformations; and 4) non-specific accumulation at the protein/bilayer interface to alter the local lipid packing, as well as 5) partitioning at the bilayer/solution interface to alter lipid bilayer properties, both of which will alter the bilayer contribution to the channel's conformational equilibrium (modified from (Andersen, 2008)).

B. Changes in bilayer properties can be determined by measuring changes in the gA monomer↔dimer equilibrium, *e.g*., (Lundbaek et al., 2010) because the ion conducting, bilayer-spanning gA channel's hydrophobic length is less than the host bilayer's hydrophobic thickness. gA channel formation thus leads to a local membrane thinning, with an associated energetic cost that varies with changes in the bilayer properties, thus making gA channels suitable probes for changes in bilayer properties.

C. Effect of 2,6-DTBP on the time course of Tl^+ quenching of ANTS fluorescence. Normalized fluorescence quench traces displaying the normalized fluorescence time signal over 1 s, gray dots denote results from all repeats ($n > 5$ per condition); red lines denote the average of all repeats. The upper two, largely flat and superimposed, traces show fluorescence quenching in the absence of gA and presence of the quencher Tl^+ in the absence and presence of 100 μM 2,6-DTBP; the lower four, exponentially decaying and essentially superimposed, traces report the

fluorescence time courses observed in gA-containing vesicles incubated with 0, 10, 20 and 100 μM 2,6-DTBP.

D. The first 100 ms of the fluorescence time courses. The dots denote results from a single repeat for each condition; the lines correspond to the stretched exponential fits (2 – 100 ms) to those repeats. The stippled line marks the 2 ms time point, at which the quenching rate is determined.

E. Fluorescence quench rates in the presence of the indicated concentrations of alkylphenols normalized to the rate determined in the agent's absence.

F. Log plot showing the EC_{50} for inhibition of HCN1 by the indicated alkylphenols.

Table 1. Relationship between total and free plasma and CSF propofol concentrations during general anesthesia

Reference	**(Engdahl et al., 1998)**		**(Dawidowicz et al., 2002)**		**(Dawidowicz et al., 2003)**		**(Dawidowicz and Kalitynski, 2003)**	
Propofol dosing[a]								
Bolus (mg/kg)	2		-		2		-	
Infusion (μg/kg/min)	133 × 15 min then 100 thereafter		-		200 × 15 min, then 150 × 30 min, then 100 thereafter		-	
Infusion TCI (μg/ml)	-		4.5 - 5 × 15 min then 3.5 - 4 thereafter		-		4.5 - 5 at induction then 3.5 - 4 thereafter	
Plasma [propofol]	**μg/ml**	**μM**[c]	**μg/ml**	**μM**[b]	**μg/ml**	**μM**[b]	**μg/ml**	**μM**[b]
Total	2.2	12.3	4.5 - 5	25.2 - 28	3.3 - 4.2	18.5 – 23.6	6.1	34.2
Free (measured)	-	-	-	-	-	-	0.06	0.34
Free (calculated)[b]	0.06	0.31	0.11 – 0.13	0.6 - 0.7	0.08 - 0.1	0.4 - 0.6	0.15	0.86
CSF [propofol]	**ng/ml**	**μM**	**ng/ml**	**μM**	**ng/ml**	**μM**	**ng/ml**	**μM**
Total	36.0	0.2	21 - 29	0.1 - 0.16	51 - 86	0.3 - 0.5	95.6	0.54
Free	-	-	-	-	-	-	-	-
Total							~78[d]	0.4
Free (measured)							~24[d]	0.1

[a] The fixed-rate dosing regimens in Engdahl *et al*. (1998) and Dawidowicz *et al*. (2003) yield comparable total propofol plasma levels as the target controlled infusion regimens employed in Dawidowicz *et al*. (2002) and Dawidowicz & Kalitynski (2003). Using the same pharmacokinetic model as the Diprofusor™ software (Dawidowicz *et al*. 2002), total effect site propofol concentration in Engdahl *et al*. (1998) is estimated to be 2.75 – 2.80 μg/ml and 3.25 – 3.30 μg/ml in Dawidowicz *et al*. (2003), both of which are in good agreement with the observed values. Our modeling is based on a 30 yr old male, height 178 cm, weight 75 kg.

[b] Calculated free [propofol] was determined assuming that the free fraction is 2.5% of the total (Servin et al., 1988).

[c] Data originally provided as mass/ml; molar concentrations calculated using propofol molecular weight = 178.3.

[d] Different group of subjects than used for measuring plasma and total CSF concentrations.

N.B. - The *total* plasma propofol concentration which typically produces loss of consciousness is on the order of 3 - 5 μg/ml (17 – 27 μM) (Smith et al., 1994) and references therein).

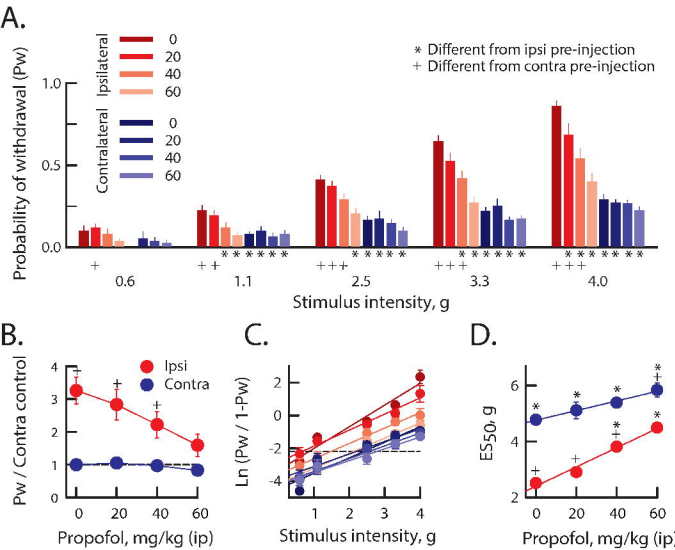
A.
Probability of withdrawal (Pw)
Ipsilateral
Contralateral
0
20
40
60
* Different from ipsi pre-injection
+ Different from contra pre-injection
1.0
0.5
0.0
0.6
1.1
2.5
3.3
4.0
Stimulus intensity, g
B.
Pw / Contra control
Ipsi
Contra
Propofol, mg/kg (ip)
C.
Ln (Pw / 1-Pw)
Stimulus intensity, g
D.
ES50, g
Propofol, mg/kg (ip)

Figure 1

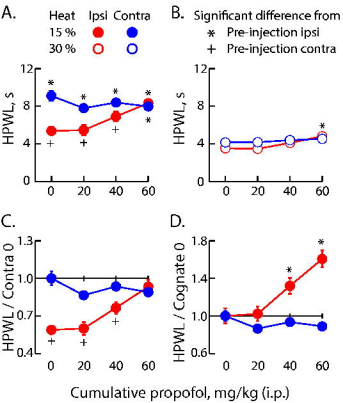
A.
Heat
Ipsi
Contra
15 %
30 %
HPWL, s
B.
Significant difference from
Pre-injection ipsi
Pre-injection contra
HPWL, s
C.
HPWL / Contra 0
D.
HPWL / Cognate 0
Cumulative propofol, mg/kg (i.p.)

Figure 2

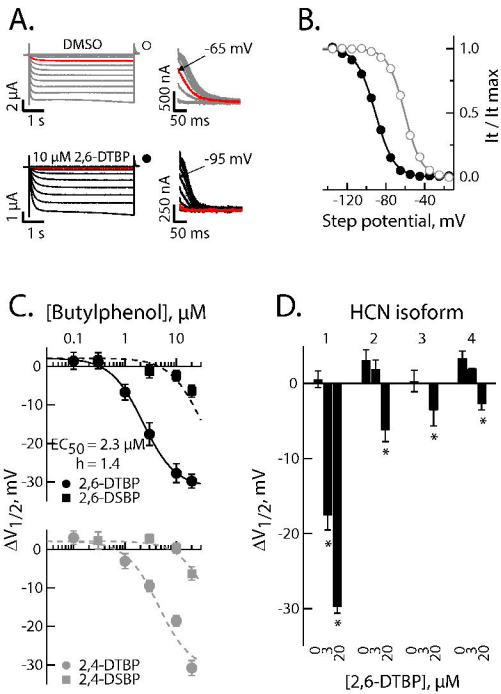
A.
DMSO
2 µA
1 s
-65 mV
500 nA
50 ms
10 µM 2,6-DTBP
1 µA
1 s
-95 mV
250 nA
50 ms
B.
1.0
0.5
0.0
It / It max
-120
-80
-40
Step potential, mV
C.
[Butylphenol], µM
0.1
1
10
0
-10
-20
-30
EC50 = 2.3 µM
h = 1.4
2,6-DTBP
2,6-DSBP
ΔV1/2, mV
2,4-DTBP
2,4-DSBP
D.
HCN isoform
1
2
3
4
ΔV1/2, mV
0
-10
-20
-30
0 3 20
[2,6-DTBP], µM

Figure 3

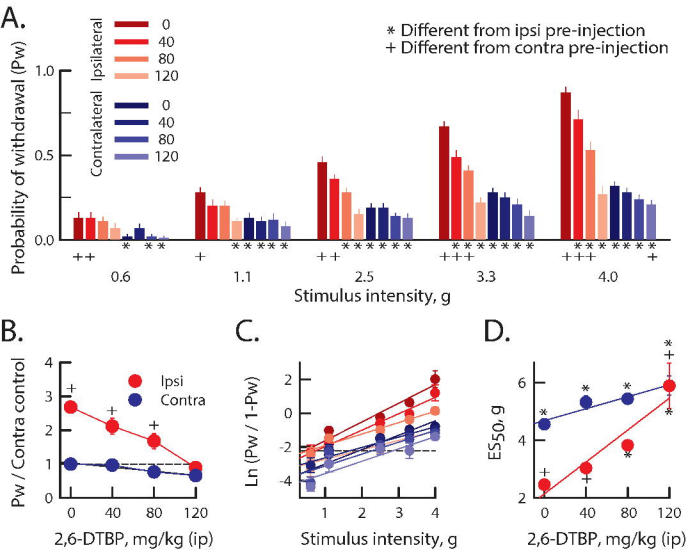
A.
Ipsilateral
0
40
80
120
Contralateral
0
40
80
120
* Different from ipsi pre-injection
+ Different from contra pre-injection
Probability of withdrawal (Pw)
1.0
0.5
0.0
++
*
* *
+
* * * * *
++
* * * * * * *
+++
* * * * * * *
+++
* * * * *
+
0.6
1.1
2.5
3.3
4.0
Stimulus intensity, g
B.
Pw / Contra control
Ipsi
Contra
2,6-DTBP, mg/kg (ip)
C.
Ln (Pw / 1-Pw)
Stimulus intensity, g
D.
ES50, g
2,6-DTBP, mg/kg (ip)

Figure 4

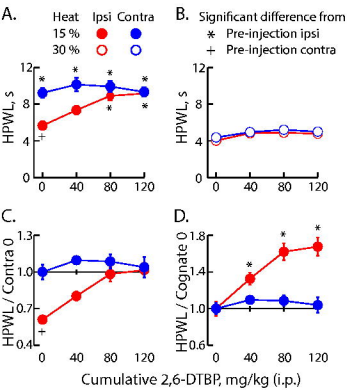
A.
Heat
15 %
30 %
Ipsi
Contra
HPWL, s
12
8
4
0
0
40
80
120
B.
Significant difference from
Pre-injection ipsi
Pre-injection contra
HPWL, s
C.
HPWL / Contra 0
1.3
1.0
0.7
0.4
D.
HPWL / Cognate 0
1.8
1.4
1.0
0.6
Cumulative 2,6-DTBP, mg/kg (i.p.)

Figure 5

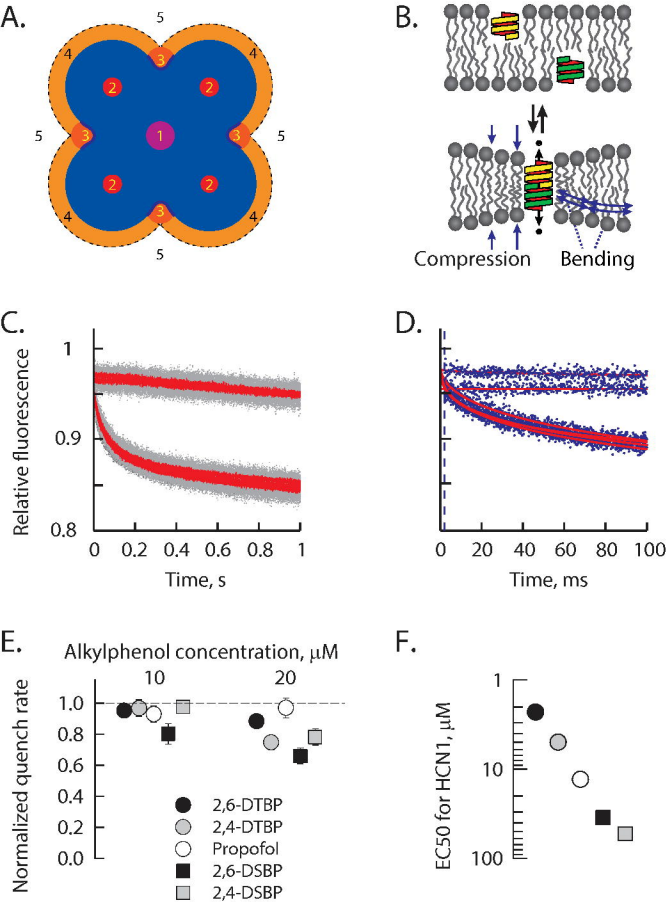
A.
B.
Compression
Bending
C.
Relative fluorescence
Time, s
D.
Time, ms
E.
Alkylphenol concentration, μM
Normalized quench rate
2,6-DTBP
2,4-DTBP
Propofol
2,6-DSBP
2,4-DSBP
F.
EC50 for HCN1, μM

Figure 6

HCN1 channels as targets for anesthetic and non-anesthetic propofol analogs in the amelioration of mechanical and thermal hyperalgesia in a mouse model of neuropathic pain

Gareth R. Tibbs, Thomas J. Rowley, R. Lea Sanford, Karl F. Herold, Alex Proekt, Hugh C. Hemmings, Olaf S. Andersen, Peter A. Goldstein, Pamela D. Flood

JOURNAL OF PHARMACOLOGY AND EXPERIMENTAL THERAPEUTICS

SUPPLEMENTAL METHODS

Solubilization of alkylphenols for in vivo and in vitro analysis For most *in vitro* experiments propofol and its dibutyl analogues were solubilized as 500 mM stock solutions in DMSO. Serial dilutions were then dispersed into the aqueous recording solutions maintaining the DMSO concentration at 0.04 % ($^{W}/_{V}$). Given that the examined concentrations approach the aqueous solubility limits of the less soluble butylphenol compounds (variously reported as 20 – 200 μM for 2,6-di-*tert*-butylphenol compared to 864-1740 μM for propofol (Brewster et al., 1994; Trapani et al., 1996) and CAS/InCHEM data sheets), recording solutions were shaken vigorously for 120 min after addition of propofol or its analogues. It has been reported that 2,6-DTBP can be prepared as an injectable 1 % ($^{W}/_{V}$) dispersion using a Cremaphor preparation (James and Glen, 1980), but our initial attempts to solubilize 2,6-DTBP using the more biologically tolerated Intralipid® emulsion (akin to the Diprivan® formulation of propofol - (Baker and Naguib, 2005)) were unsuccessful. Thus, we found that even if the 2,6-DTBP was liquefied by heating to 60 ^{o}C prior to addition of intralipid and the mixture shaken vigorously

for 1-18 hours, the combination was always recovered in two phases, a yellow oily accumulation and a white emulsion. In contrast, we found 2,6-DTBP could be solubilized at 1% ($^{W}/_{V}$) in a carrier solution of 40% ($^{W}/_{V}$) dihydroxy-ß-cyclodextrin (DHßCD, a biologically tolerated carrier (Brewster et al., 1990)) using a simple, standardized, protocol.

To this end, appropriate masses of 2,6-DTBP and DHßCD that would yield 6 ml of 1% 2,6-DTBP in combination with 40% DHßCD were combined in a Teflon® capped borosilicate vial and heated to 60 ^{o}C in a water bath. This temperature is above the melting point of 2,6-DTBP (36 ^{o}C (Lorenc et al., 2003)) but below that of DHßCD (>200 ^{o}C (Loftsson and Brewster, 1996)) and is compatible with stability of both reagents ((Loftsson and Brewster, 1996; Lorenc et al., 2003) and CAS documentation). After 15 min the molten 2,6-DTBP was intimately mixed with the DHßCD by vigorous vortexing, 200 µL of 60 ^{o}C deionized (DI) H_2O added and, following additional vortexing, the vial returned to the water bath for 15-30 min. Following addition of 3 further 200 µL aliquots of DI H_2O, with corresponding incubation and vortexing, the sample was left at 60 ^{o}C overnight. The resulting colorless viscous gel was slowly diluted by addition of the required volume of DI H_2O adding no more than 200 µL at a time with 15-30 min incubation at 60 ^{o}C and vortexing after each addition. The resulting clear, colorless, solution could be stored at -20 ^{o}C with no phase separation or precipitation. Visual observation upon dispersal of this co-solution into an aqueous phase was consistent with aqueous solvation rather than precipitation of the 2,6-DTBP. If DHßCD were omitted, after the overnight incubation 2,6-DTBP was present as yellow oily droplets akin to those observed when the compound was dispersed in the presence of Intralipid®.

Gas chromatography analysis of 2,6-DTBP Gas chromatography (GC) was performed according to a modification of a method for propofol analysis (Yu and Liau, 1993; Fan et al.,

1995) using a Shimadzu GC-2010 Plus gas chromatograph (Shimadzu, Kyoto, Japan) equipped with a split/splitless injection unit, a forensic crossbond phase fused silica column (Rtx-BAC2, 25 m x 0.53 mm, 2 μm film thickness, Restek U.S., Bellefonte, PA) and a flame ionization detector (FID). The injection port and FID were at 280 ˚C while the column temperature was 210 ˚C. The split ratio was 2:1 while the column flow was 6.96 ml/min with helium (linear velocity 65 cm/s). Samples and standards were prepared as follows. To 200 μL of whole blood (drawn following injection of HPβCD or 2,6-DTBP solubilized in HPβCD), we added 200 μL of chloroform containing 100 nM thymol as internal standard and 2 μL of DMSO. Following mixing (vortex for 20 s followed by 30 min on a rotator) and subsequent centrifugation (5000 g for 10 min at 10 ˚C), the chloroform phase was transferred into a glass GC vial and washed with an equal volume of 0.5 M NaOH. To compare 2,6-DTBP acutely solubilized in DMSO with 2,6-DTBP solvated in HPβCD (according to our standard protocol), we combined an aliquot of the appropriate solution containing 10 nmoles of 2,6-DTBP with 200 μL chloroform containing the thymol internal standard (an addition that would result in a concentration of 50 μM 2,6-DTBP in the chloroform phase if all the 2,6-DTBP partitions therein). HPβCD was added to the DMSO-solubilized 2,6-DTBP sample and DMSO was added to the HPβCD-solubilized 2,6-DTBP sample so that the final concentrations of HPβCD and DMSO were equivalent. An equal volume of H_2O was added, the samples mixed vigorously, then the chloroform phase recovered as described above. A control without 2,6-DTBP was processed in parallel. For the standard calibration curve, aliquots of 2,6-DTBP acutely solubilized in DMSO were added to 200 μL of chloroform plus the thymol internal standard (total DMSO addition was 2 μL in all cases). We then added 200 μL of H_2O and processed the samples as described above. In order to determine the extraction efficiency from blood, 2,6-DTBP-spiked mouse

whole blood samples were processed using the extraction method above. Extraction efficiency was calculated to be 0.42; therefore a correction factor of 2.39 was applied to measurements from whole blood samples. In all cases 2 µL of the chloroform phase were injected for analysis. Representative chromatograms and calibration curves are shown in Figures S1 and S2.

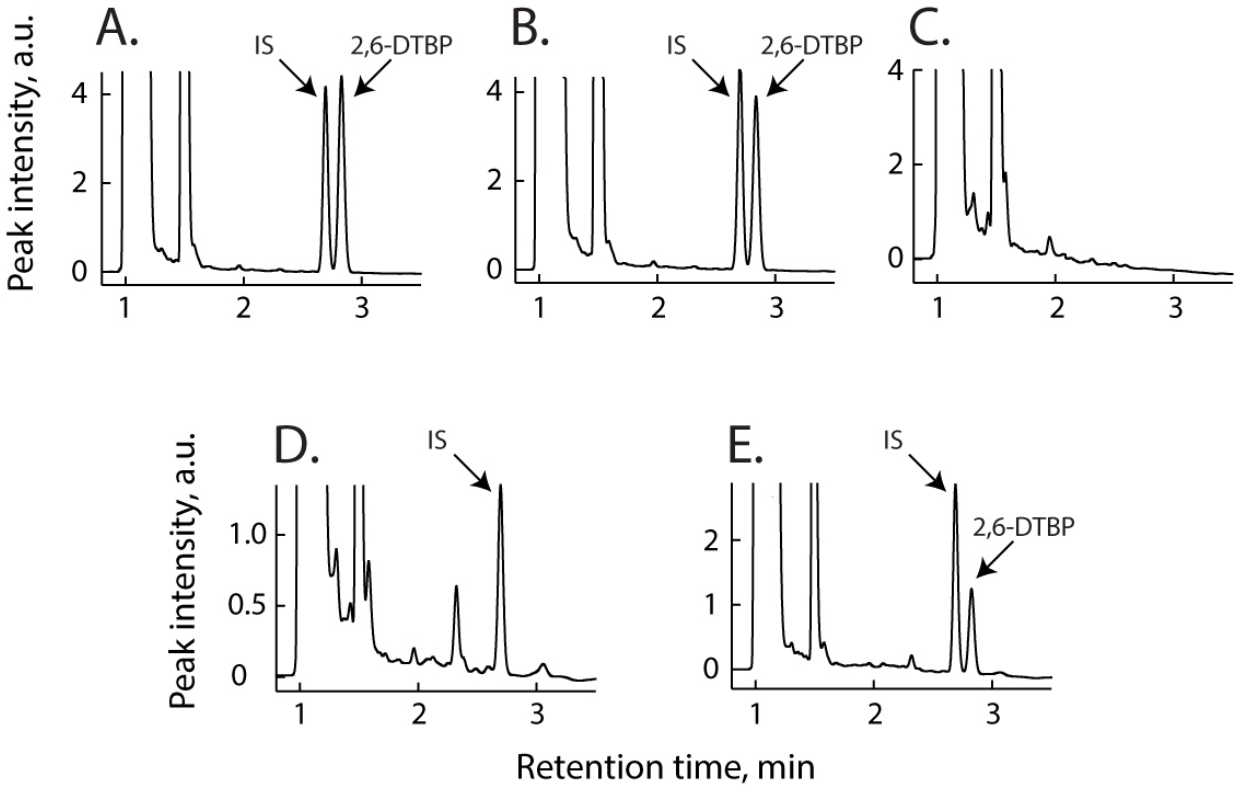

Figure S1. Gas chromatography of DHßCD solubilized 2,6-DTBP.
A-C. Representative GC chromatograms of 2,6-DTBP solubilized acutely in DMSO (**A**) or following solvation in HPβCD (**B**) with respect to a sample containing both DMSO and HPβCD but not 2,6-DTBP (**C**). The first large peak at 1 min retention time (RT) is the solvent chloroform followed by a DMSO peak at ~1.5 min. The peak of the thymol internal standard (IS, 2.7 min RT, 100 nmol) is in close proximity of the 2,6-DTBP peak (2.8 min RT). Note that, for clarity, the thymol internal standard was omitted from the sweep in panel **C**.

D,E. Representative GC chromatograms of extracts taken from whole blood following injection with HPβCD vehicle (**D**) or 80 mg/kg (*i.p.*) 2,6-DTBP in HPβCD (**E**). The total 2,6-DTBP concentration in blood was 24 µM ± 11 (mean ± SEM), n = 6.

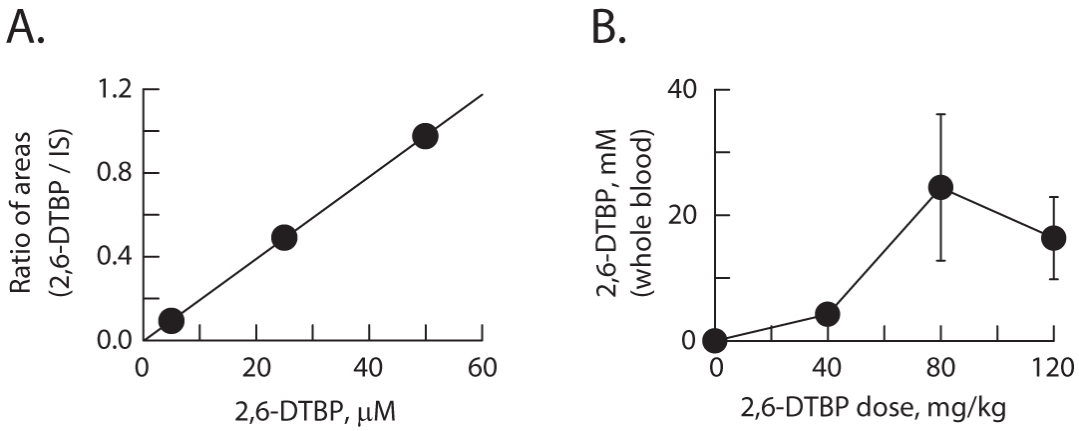

Figure S2. Bioavailability of DHßCD solubilized 2,6-DTBP.

A. Representative standard curve for 2,6-DTBP and the internal standard. Each point is mean ± SEM for triplicate determinations.

B. Whole blood concentrations of 2,6-DTBP observed following the indicated cumulative dose of alkylphenol. Each point represents mean ± SEM from 5 or 6 mice.

SUPPLEMENTAL RESULTS AND DISCUSSION

Thermal stability of DHßCD solubilized 2,6-DTBP Alkylphenols are subject to oxidation (Hassanein et al., 1994) yielding, for example, quinones or dimerized DTB hydroxyquinones (Bedell and Martell, 1983; Wang et al., 1984; Fujiyama et al., 1999); such compounds are biologically available and bioactive (*e.g.*, probucol and succinobucol (Wasserman et al., 2003; Stocker, 2009)). This raises the possibility that there could be marked transformation of 2,6-DTBP during HPβCD solvation. Comparison of the chromatograms in Figure S1 suggests this is unlikely to be a significant factor. Thus, chromatograms of 2,6-DTBP dissolved in DMSO immediately prior to GC analysis (Fig. S1A) are essentially identical to those of HPβCD solvated 2,6-DTBP (Fig. S1B). Compare both to Fig. S1C wherein vehicles without 2,6-DTBP were analyzed – note that the thymol standard was omitted here for clarity. These findings are consistent with DHßCD exerting a protective effect on compounds caged within the cyclodextrin structure (Brewster et al., 1994; Loftsson and Brewster, 1996). Furthermore, our observations that DHßCD and DMSO solubilized 2,6-DTBP are equally effective as antagonists of HCN1 support the contention that there is little or no loss of 2,6-DTBP during its solubilization in the presence of the excipient, DHßCD. These results do not exclude the possibility that a low abundance contaminant of our 2,6-DTBP accounts for the biologically relevant analgesic activity, but they argue against such a compound arising during formulation.

A second concern with our formulation involves the use of DHßCD for 2,6-DTBP but Intralipid® for propofol. If these vehicles result in markedly different pharmacokinetic and pharmacodynamic behaviors, the relative efficacy of the agents might be poorly reflected in our behavioral data. We do not think that this is the case for the following reasons: first, the

pharmacokinetics and pharmacodynamics of propofol solvated in DHßCD are indistinguishable from propofol dispersed in Intralipid® or Cremaphor supporting the notion that DHßCD functions as a reliable vehicle for *in vivo* dispersal of the butylphenol analogues (Viernstein et al., 1993; Trapani et al., 1998; Egan et al., 2003); second, the whole blood concentrations of 2,6-DTBP we observed are those expected if propofol and 2,6-DTBP have similar pharmacokinetic properties irrespective of vehicle; third, DHßCD solubilized 2,6-DTBP is comparable to 2,6-DTBP solubilized in DMSO as an HCN1 antagonist, which supports the notion that the caged compound is readily aqueous available upon dilution; and fourth, as 2,6-DTBP achieved essentially full analgesic efficacy, the key effect of a dispersal error would be to underestimate its potency and not yield a false positive.

Bioavailability of DHßCD solubilized 2,6-DTBP Is DHßCD solvated 2,6-DTBP readily bioavailable and what are the blood concentrations during the behavioral testing window? To address this question, we injected animals with increasing doses of our standard 2,6-DTBP/HPβCD formulation or HPβCD alone, recovered whole blood by venous puncture then processed the samples for GC as described in Supplemental Methods. Figure S1D and E show chromatograms obtained from samples wherein animals had received HPβCD or a cumulative dose of 80 mg/kg 2,6-DTBP (two 40 mg/kg doses administered at the normal timing protocol). Injection of 2,6-DTBP yielded a peak with the characteristic retention time of the alkylphenol. The whole blood concentration of 2,6-DTBP for a cumulative dose of 80 mg/kg was 24 μM ± 11 (mean ± SEM, n = 6). Figure S2B shows the whole blood concentration of 2,6-DTBP as a function of the cumulative administered dose. The behavior accords with *i.p.* HPβCD solvated 2,6-DTBP had similar pharmacokinetic and pharmacodynamic behavior as *i.p.* propofol.

Toxicity of DHßCD solubilized 2,6-DTBP It has previously been reported that 2,6-DTBP is well tolerated following acute exposure to intravenous doses of 80-100 mg/kg (James and Glen, 1980). Although the absolute dose is roughly comparable to that used in our behavioral studies, the blood concentration achieved through intravenous injection is likely to be some 40-fold greater than that achieved in our behavioral tests. Such findings suggest 2,6-DTBP is not acutely toxic. To gain further insight into toxicity associated with the elevated systemic load consequent upon use of *i.p.* injection, we exposed four mice to a single bolus dose of 80 mg/kg, a dose that appears to offer a near maximal therapeutic relief. In agreement with James and Glen (James and Glen, 1980), all mice tolerated this dose well, and they survived for the seven day post-2,6-DTBP observation window during which time their behavior was indistinguishable from paired controls.

Validation of mechanical and thermal behavioral assays with respect to development of neuropathic pain following nerve ligation For discussion of Figures S3 and S4, see the main text.

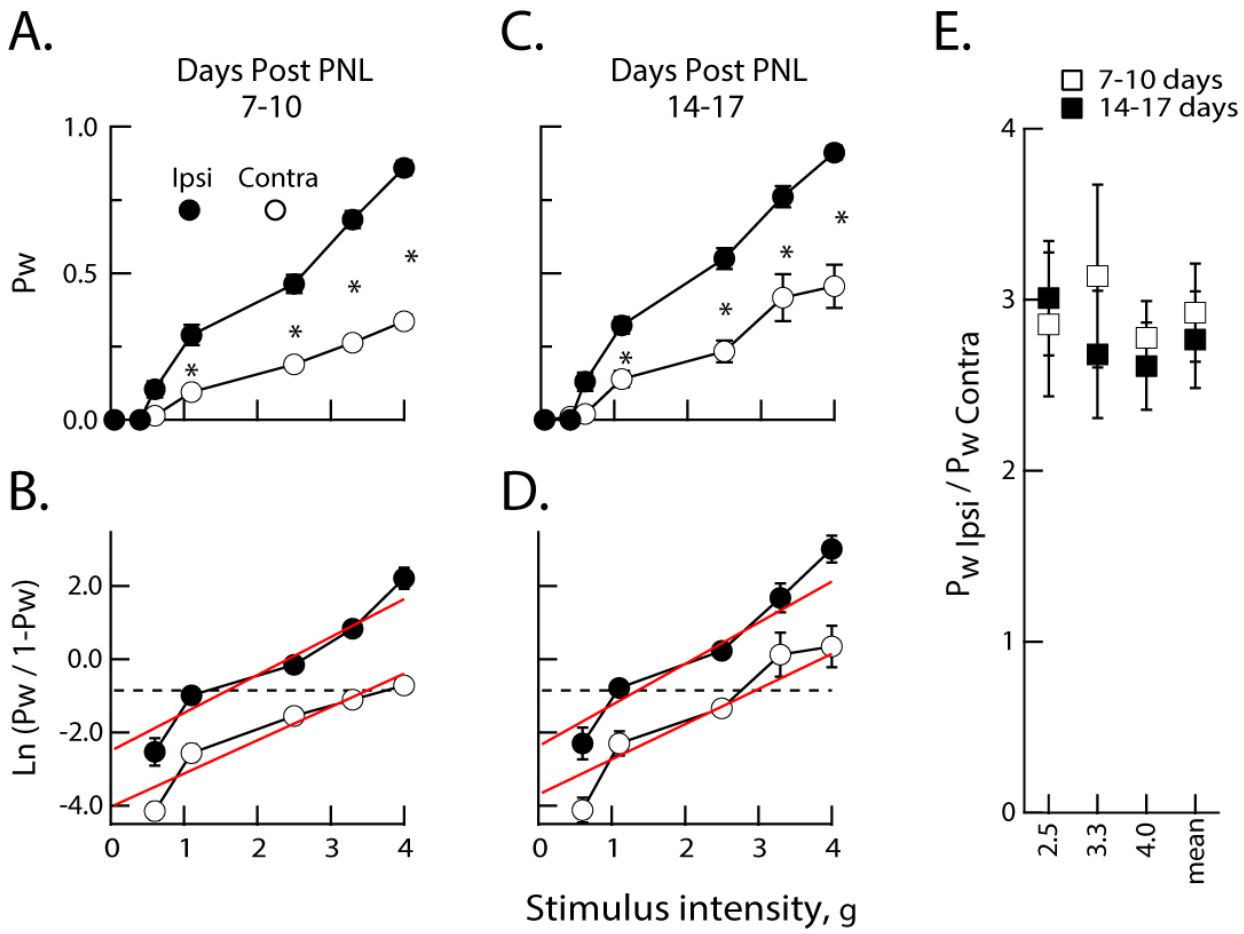

Figure S3: Von Frey fiber analysis of mechanical hyperalgesia as a function of time post-PNL and stimulus strength.

A-D. Probability of paw withdrawal (P_W) as a function of stimulus fiber strength (**A,B**) and a Logit transformation (ln [P_W / 1-P_W]) thereof (**C,D**) at 7-10 (**A,C**) or 14-17 (**B,D**) days post-PNL. In **B** and **D**, the red lines represent linear regressions to the mean data while the dashed lines represent a P_W of 0.3. Asterisks indicate those pairs of $P_{W,IPSI}$ and $P_{W,CONTRA}$ that are statistically different.

E. Ratio of $P_{W,IPSI}$ to $P_{W,CONTRA}$ observed in response to the indicated fiber strengths and the mean thereof as a function of time post-PNL. P_W ratios determined in response to each fiber and the mean thereof were not significantly different from each other within or between the two time points.

Data for 7 - 10 and 14 - 17 days are from 19 and 18 animals respectively (except for 0.6 g stimuli which were from 10 animals.

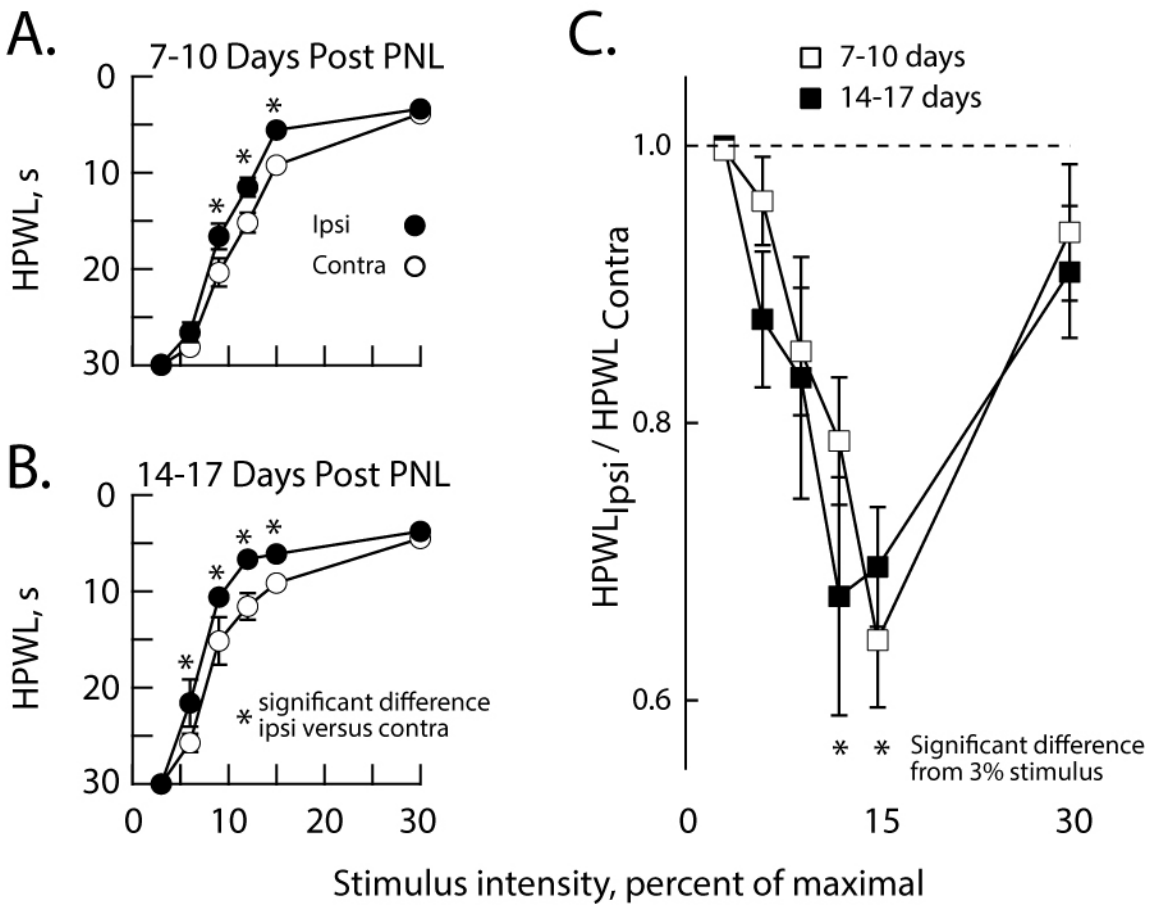

Figure S4: HPWL analysis of thermal hyperalgesia as a function of time post-PNL and stimulus strength.

A,B. HPWL as a function of stimulus heat source intensity determined 7-10 or 14-17 days post-PNL. $HPWL_{IPSI}$ is significantly different from $HPWL_{CONTRA}$ at intermediate stimulus strengths (9 - 15% at 7 - 10 days and 6 - 15% at 14 - 17 days – A and B, respectively) but not at lower intensities nor at 30%.

C. $HPWL_{IPSI}$ as a function of the stimulus intensity and time post-PNL matched $HPWL_{CONTRA}$. At both 7 - 10 and 14 - 17 days post-PNL the ratios at 12 and 15% stimulus intensity were significantly different (asterisked) from that observed at 3% but ratios determined at the same intensity were not different between the two trial times.

At 7-10 days data are from 21 mice at 15% with 17 of these analyzed at all other intensities. At 14 - 17 days data are from 17 mice at 15 and 30% with four of these analyzed at 1the other intensities.

Sensitivity of the thallium quench assay as a detector of bilayer-modifying efficacy We show that the rate of gA-mediated Tl^+-induced fluorescent quenching is largely (butylphenols) or completely (propofol) insensitive to the presence of alkylphenols (Fig. 6). This behavior is in marked contrast to the action of our positive control, capsaicin. As shown in Figure S5, capsaicin elicits a concentration dependent acceleration of the fluorescence quench kinetics and a marked enhancement of the extent of quenching achieved during the assay observation period (modified from (Ingólfsson and Andersen, 2010); note the difference in scaling of the ordinate in both panels of this figure compared to those in the plots shown in Figure 6C &D).

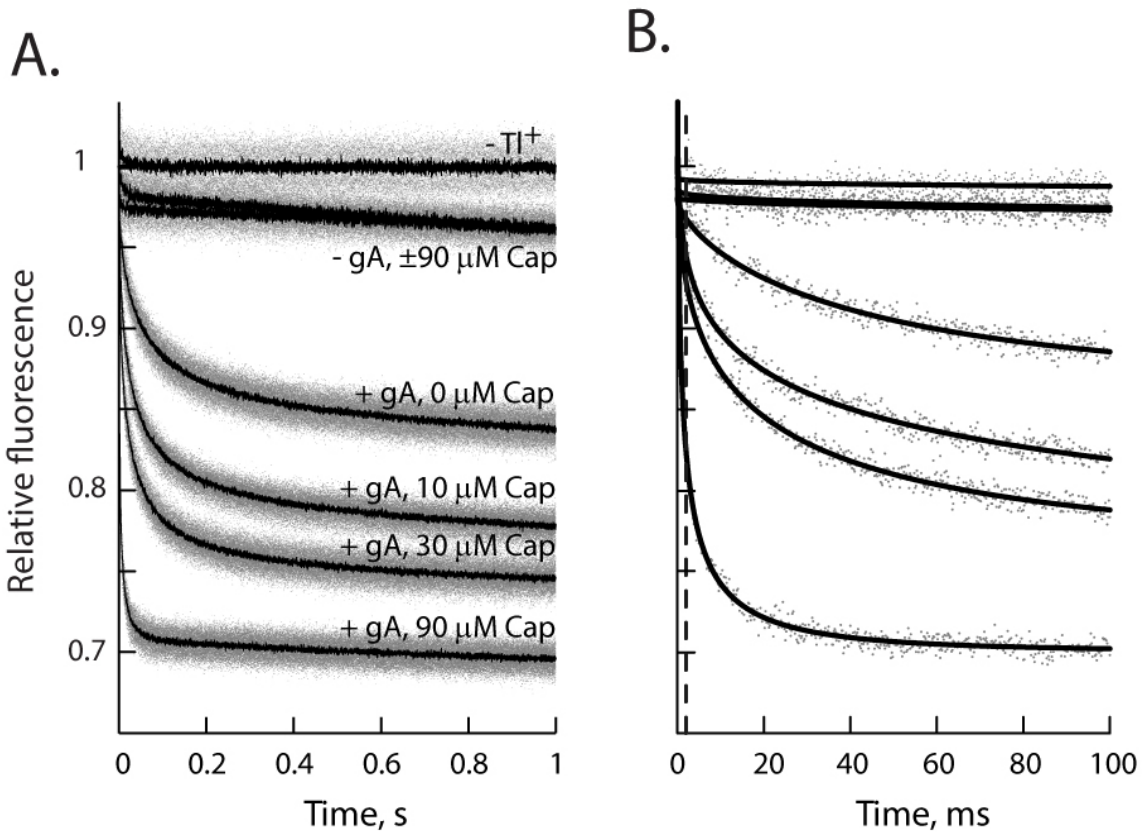

Figure S5. The behavior of a strongly bilayer-modifying agent on the gramicidin-based fluorescence assay.

A. Time course of gA-mediated fluorescence quenching by Tl^+. Data were normalized to the fluorescence signal in the absence of gramicidin and Tl^+. Gray dots denote results from all repeats ($n > 5$ per condition); the black lines denote the average of all repeats. The presence or absence of gA, Tl^+ and varying concentrations of capsaicin (Cap) are indicated next to the appropriate traces. Note, in the absence of gA, the time course of quenching in the absence or presence of the highest concentration of capsaicin is essentially superimposed.

B. The initial 100 ms of representative fluorescence quench time courses. Here, the dots denote results from a single repeat for each condition while the lines correspond to the fits of the stretched exponential function. The stippled line is at 2 ms, the start time for the fit and the time at which the quench rate is calculated.

References

Baker MT and Naguib M (2005) Propofol: the challenges of formulation. *Anesthesiology* 103:860-876.

Bedell SA and Martell AE (1983) Oxidation of 2,6-di-*tert*-butylphenol by molecular oxygen. Catalysis by tetrakis(bipyridyl)(m-peroxo)(m-hydroxo)dicobalt(III). *Inorganic Chemistry* 22:364-367.

Brewster ME, Braunstein AJ, Bartruff MSM, Kibbey C, Huang M-J, Pop E and Bodor N (1994) Solubilization and electrochemical stabilization of substituted phenols through the use of 2-hydroxypropyl-β-cyclodextrin. *Supramolecular Chemistry* 4:69-76.

Brewster ME, Estes KS and Bodor N (1990) An intravenous toxicity study of 2-hydroxypropyl-ß-cyclodextrin, a useful drug solubilizer, in rats and monkeys. *Int J Pharm* 59:231-243.

Egan TD, Kern SE, Johnson KB and Pace NL (2003) The pharmacokinetics and pharmacodynamics of propofol in a modified cyclodextrin formulation (Captisol) versus propofol in a lipid formulation (Diprivan): an electroencephalographic and hemodynamic study in a porcine model. *Anesth Analg* 97:72-79.

Fan SZ, Yu HY, Chen YL and Liu CC (1995) Propofol concentration monitoring in plasma or whole blood by gas chromatography and high-performance liquid chromatography. *Anesth Analg* 81:175-178.

Fujiyama H, Kohara I, Iwai K, Nishiyama S, Tsuruya S and Masai M (1999) Liquid-Phase Oxidation of 2,6-Di-*tert*-butylphenol with Cu-Impregnated MCM-41 Catalysts in the Presence of Alkali Metals. *J Catalysis* 188:417-425.

Hassanein M, Selim A and El-Hamshary H (1994) Oxidation of 2,6-di-*tert*-butylphenol by molecular oxygen catalyzed by tetrasodium phthalocyaninatocobalt(II)tetrasulfonate bound to a polymer colloid. *Macromolecular Chemistry Physics* 195:3845-3854.

Ingólfsson HI and Andersen OS (2010) Screening for small molecules' bilayer-modifying potential using a gramicidin-based fluorescence assay. *Assay Drug Develop Technol* 8:427-436.

James R and Glen JB (1980) Synthesis, biological evaluation, and preliminary structure-activity considerations of a series of alkylphenols as intravenous anesthetic agents. *J Med Chem* 23:1350-1357.

Loftsson T and Brewster ME (1996) Pharmaceutical applications of cyclodextrins. 1. Drug solubilization and stabilization. *J Pharmaceut Sci* 85:1017-1025.

Lorenc JF, Lambeth G and Scheffer W (2003) Alkylphenols, in *Kirk-Othmer Encyclopedia of Chemical Technology* pp 203-233, John Wiley & Sons, Inc.

Stocker R (2009) Molecular mechanisms underlying the antiatherosclerotic and antidiabetic effects of probucol, succinobucol, and other probucol analogues. *Curr Opin Lipidol* 20:227-235.

Trapani G, Latrofa A, Franco M, Lopedota A, Sanna E and Liso G (1998) Inclusion complexation of propofol with 2-hydroxypropyl-b-cyclodextrin. Physicochemical, nuclear magnetic resonance spectroscopic studies, and anesthetic properties in rat. *J Pharmaceutical Sci* 87:514-518.

Trapani G, Lopedota A, Franco M, Latrofa A and Liso G (1996) Effect of 2-hydroxypropyl-ß-cyclodextrin on the aqueous solubility of the anaesthetic agent propofol (2,6-diisopropylphenol) *Int J Pharm* 139:215-218.

Viernstein H, Stumpf C, Spiegl P and Reiter S (1993) Preparation and central action of propofol/hydroxypropyl-beta-cyclodextrin complexes in rabbits. *Arzneimittelforschung* 43:818-821.

Wang XY, Motekaitis RJ and Martell AE (1984) Metallotetraphenylporphyrin-catalyzed oxidation of 2,6-di-*tert*-butylphenol. *Inorganic Chemistry* 23:271-275.

Wasserman MA, Sundell CL, Kunsch C, Edwards D, Meng CQ and Medford RM (2003) Chemistry and pharmacology of vascular protectants: a novel approach to the treatment of atherosclerosis and coronary artery disease. *Am J Cardiol* 91:34A-40A.

Yu HY and Liau JK (1993) Quantitation of propofol in plasma by capillary gas chromatography. *J Chromatogr* 615:77-81.